Rapid turnover of sex chromosomes is associated with speciation in Neotropical armored catfish *Harttia* (Siluriformes, Loricariidae)

Francisco de Menezes Cavalcante Sassi[1, 2, 3], Fernando Henrique Santos de Souza[2, 4], Foyez Shams[3], Manolo Fernandez Perez[5], Tariq Ezaz[3], Geize Aparecida Deon[2, 3], Luohao Xu[1], Marcelo de Bello Cioffi[2]

[1] MOE Key Laboratory of Freshwater Fish Reproduction and Development, College of Life Sciences, Southwest University, Chongqing 400715, China.

[2]Laboratory of Evolutionary Cytogenetics, Universidade Federal de São Carlos, São Carlos – SP 13565-905, Brazil.

[3]Institute for Applied Ecology, University of Canberra, Canberra – ACT 2617, Australia.

[4] Department of Zoology, Faculty of Science, Charles University, Prague 12800, Czech Republic.

[5]Real Jardín Botánico – RJB-CSIC, Madrid 28014, Spain.

Abstract

The genus *Harttia* represents an important repository of multiple sex chromosomes, as they are found in more than a quarter of its valid species, exhibiting distinct degrees of heteromorphism. However, little is known about the evolution of these systems from a molecular perspective. In this study, we generated DArTseq data for 17 species of *Harttia* and one outgroup species (*Farlowella* sp.) to investigate the genomic architecture underlying sex chromosome evolution in this highly dynamic genus. The time-calibrated phylogeny based on 1,381 SNPs per species (24,858 SNP markers in total) revealed three well-supported clades, with divergence between clades occurring approximately 6 to 10 million years ago (Mya), coinciding with the formation of the Amazon River and several other river capture events in South America. The reconstruction of ancestral areas and karyotype, combined with the identification of shared and specific sex-linked markers, suggests that the *Harttia* ancestor occupied either the South and Southeast Atlantic drainages or the Eastern Amazon, with a karyotype of 2n = 58 and a homomorphic XY system. Our findings suggest a recent and independent emergence of two distinct multiple sex chromosome systems at ~5 Mya for X_1X_2Y and ~1 Mya for XY_1Y_2, which is proposed to accelerate speciation rates in the genus. Together, these findings underscore the potential contribution of multiple sex chromosome systems and their turnovers in accelerating speciation rates in teleosts.

Keywords: SNP, phylogenetics, DArT-seq, sex-linked markers, probabilistic modeling

1. Introduction

In the canonical model of sex chromosome evolution, the emergence of a sex-determining gene is followed by the suppression of recombination around this locus, allowing the accumulation of sexually antagonistic alleles and other sex-linked sequences (Muller, 1918; Ohno, 1966). Structural rearrangements of chromosomes, such as inversions, might further consolidate this recombination suppression, resulting in the gradual differentiation and heteromorphy of the sex chromosomes (Graves, 2006). Nonetheless, before these chromosome rearrangements in regions where recombination persists, such as the pseudoautosomal region (PAR), sex-linked loci may still recombine between the X and Y or Z and W chromosomes (Zhu et al., 2025). These dynamics are particularly relevant in species exhibiting homomorphic sex chromosomes, where recombination suppression may be either partial or recent (reviewed in Charlesworth, 2017). Comprehending the inheritance patterns, chromosomal locations, and evolutionary trajectories of sex-linked markers is crucial for elucidating the origins and diversity of sex-determination systems (Kratochvíl et al., 2021; Zhu et al., 2025).

Multiple sex chromosome systems originate from chromosomal rearrangements that occur in simple systems (XX/XY or ZZ/ZW). These rearrangements may involve fissions of ancestral chromosome pairs or fusions with autosomes and are generally considered rare in eukaryotes (White, 1940; Kitano and Peichel, 2012; Pokorná et al., 2014; Pennell et al., 2015), found in only about 100 fish species (reviewed in Sember et al., 2021; Wang et al., 2022). However, our understanding of the evolution of sex chromosomes remains largely shaped by studies conducted in a limited number of model organisms, which typically possess heteromorphic sex chromosomes at

advanced evolutionary stages, thus providing a restricted view of the diversity and complexity of sex determination systems found in nature (Zhu et al., 2025).

In this context, the Neotropical armored catfish *Harttia* (Siluriformes: Loricariidae) is emerging as an exceptional model system to study multiple sex chromosomes with distinct degrees of degeneration. Comprising 28 valid species (Fricke et al., 2025), this monophyletic genus (Rapp Py-Daniel, 1997; Covain et al., 2016; Londoño-Burbano and Reis, 2021) is distributed across rheophilic habitats of the Brazilian and Guiana Shields. *Harttia* exhibits the highest number of multiple sex chromosome systems among fish, with about 28% of species displaying heteromorphic sex chromosomes (Sassi et al., 2024), a proportion matched only by *Notobranchius* killifishes (Krysanov and Demidova, 2018; Štundlová et al., 2022; Hospodářská et al., 2025). These systems vary in complexity and differentiation, making *Harttia* a unique model for studying repeated sex chromosome turnover and the independent origins of multiple sex chromosome systems. Conventional and molecular cytogenetic data revealed an exceptional diversity of 2n (from 52 to 62 chromosomes) and two independent male-heterogametic systems (**Figure 1, also Figure 5 with new results**): the XX/XY_1Y_2 and its homologous XX/XY in species from South and Southeast Brazil, and the $X_1X_1X_2X_2/X_1X_2Y$ system with a corresponding XX/XY in Amazonian species (Centofante et al., 2006; Blanco et al., 2014; Sassi et al., 2020; Deon et al., 2020). The rare XX/XY_1Y_2 system, described for only nine fish species to date (reviewed in Deon et al., 2020), is found in three *Harttia* species: *H. carvalhoi* and *Harttia* sp. 1, originating from a sex chromosome-autosome translocation (SC-A) involving an ancestral XX/XY configuration (seen in *H. torrenticola*), with a subsequent reciprocal translocation with an additional autosomal pair giving rise to the XX/XY_1Y_2 seen in *H. intermontana* (Centofante et al., 2006; Deon et al., 2020, 2022a,b). Conversely, in the Amazonian

lineage, a fission of the ancestral XY system (likely the same seen in *H. rondoni*) is proposed to have led to the emergence of the X_1X_2Y system found in *H. duriventris*, *H. villasboas*, and *H. punctata* (Sassi et al., 2023a, b). Comparative analyses of satellite DNA content further reveal distinct degrees of differentiation among these systems, indicating multiple independent origins and divergent evolutionary trajectories (Deon et al., 2024; Sassi et al., 2025).

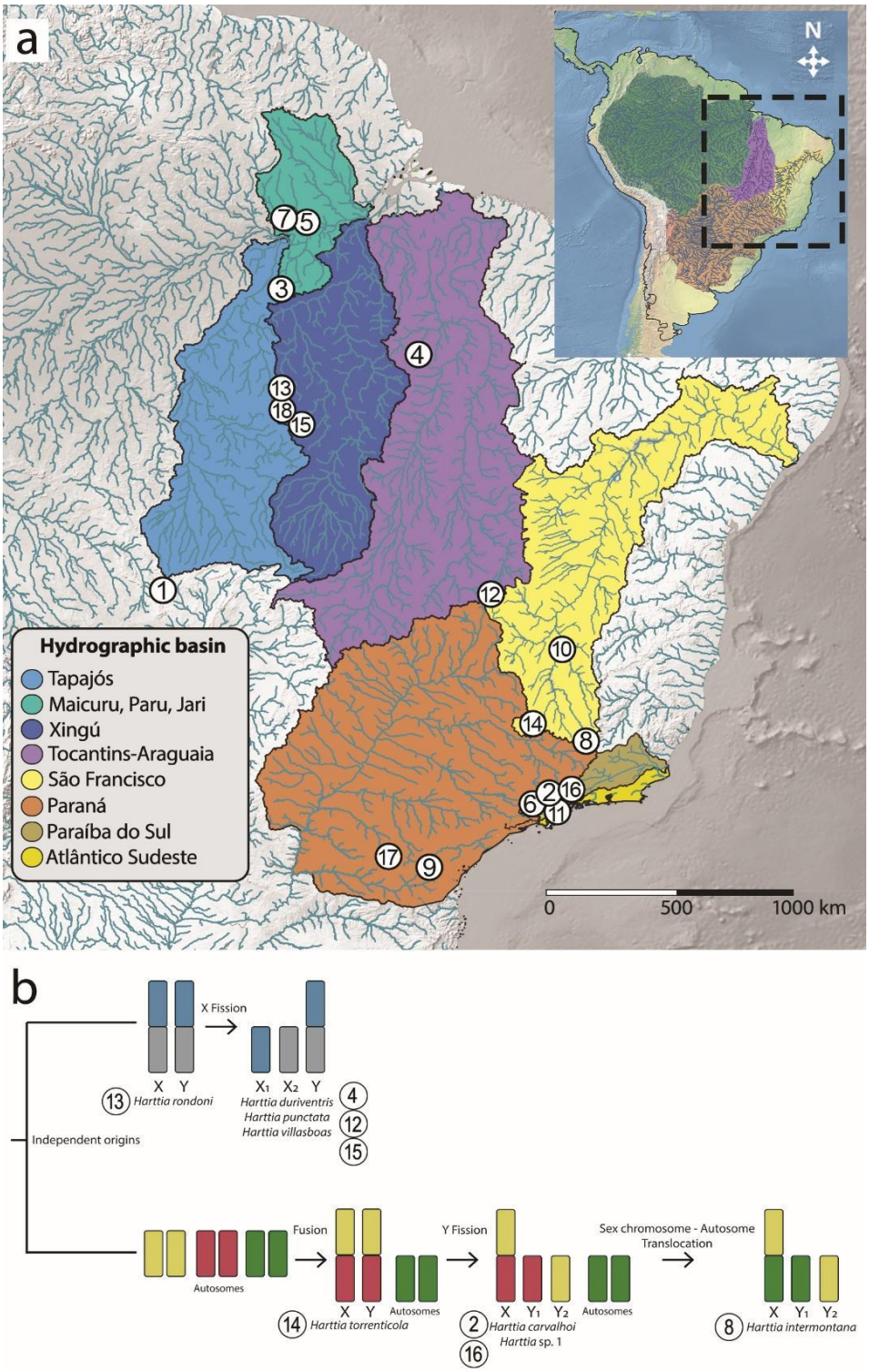

Figure 1. a) Partial Brazilian map indicating sample sites (circles) and river basins (colored areas). Numbering follows **Supplementary Table 1.** The upper right corner map shows the Neotropical region (black contour line), and the four main basins: Amazon (dark green), Tocantins-Araguaia (purple), La Plata (orange), and São Francisco (yellow). **b)** Schematic view of the proposed evolutionary pathways of *Harttia* sex chromosomes, based on previous cytogenetic data from Centofante et al. (2006), Blanco et al. (2014), Deon et al. (2020, 2022a, b, 2024), and Sassi et al. (2020, 2021, 2023a, b, 2025).

110 Without the availability of a reference genome, complexity reduction techniques
111 have proven to be powerful tools for genomic research in non-model organisms (e.g.,
112 Nedoluzhko et al., 2021; Kirschner et al., 2022; Suchan et al., 2024; Knief et al., 2024).
113 These approaches offer a cost-effective means of generating thousands of molecular
114 markers, suitable for investigating genetic polymorphisms, assessing population
115 structure, and exploring patterns of genome evolution (Davey et al., 2011). Analyses
116 using large nuclear marker datasets provide higher resolution and assist in overcoming
117 issues such as incomplete lineage sorting and restricted taxon sampling (Mirarab et
118 al., 2016; Simmons & Gatesy, 2021). DArTseq (Diversity Arrays Technology
119 sequencing) (Jaccoud et al., 2001) has emerged as a widely used method due to its
120 ability to target low-copy and predominantly active genomic regions, which may include
121 sex-specific loci, before high-throughput sequencing (Wenzl et al., 2004). These
122 features have enabled DArTseq applications in a broad range of taxa and research
123 areas, including genetic diversity, hybridization, admixture, phylogeography,
124 phylogenetics, and the identification of sex-linked markers (Lambert et al., 2016;
125 Baloch et al., 2017; Melville et al., 2017; Alam et al., 2018; Sopniewski et al., 2019;
126 Aznar-Fernández et al., 2020; Mujyambere et al., 2024). Sex-linked markers provide
127 key insights into the localization and structure of sex-determining regions, offering a
128 molecular entry point into the evolutionary processes that shape sex chromosome
129 systems (Lambert et al., 2016).
130 In this current study, we performed DArTseq in 17 *Harttia* species and one outgroup
131 species (*Farlowella* sp.) to examine the genomic architecture of sex chromosome
132 evolution in this dynamic genus (**Supplementary Table 1**). Our primary objective was
133 to identify the likely mechanisms underlying the diversity of multiple sex chromosomes
134 in the genus. To this end, we focused on identifying putative sex-linked markers and

analyzing their distribution across species with different sex chromosome systems. A comprehensive phylogenetic tree based on SNP data was constructed, integrating spatial and cytogenetic information by reconstructing ancestral distribution areas and modeling chromosome number evolution using probabilistic approaches. Our findings indicate that the rapid turnover of multiple sex chromosome systems, originating from an ancestral XY configuration, may be linked to an accelerated tempo of diversification in *Harttia.*

144 **2. Results**

145 ***2.1 Evolutionary relationships in Harttia***

146 A total of 95,305 SNPs and 282,275 SilicoDArT (presence and absence) loci
147 were generated for 107 individuals from 17 *Harttia* and one *Farlowella* species. The
148 resulting phylogeny, constructed using 1,381 SNP loci per species (24,858 SNP
149 markers in total) after stringent filtering, grouped all *Harttia* species into three primary
150 clades, each exhibiting strong geographic coherence (**Figure 2a**). Exceptionally,
151 *Harttia* sp. 2 was placed as a single ancestral branch to all remaining *Harttia*, not
152 included in any of the three clades. Clade I comprises species from the Guiana Shield
153 drainages (*H. fowleri* and *H. guianensis*). At the same time, Clade II included species
154 from Amazon Brazilian Shield drainages, specifically the Xingu, Tapajós, and
155 Tocantins-Araguaia River Basins (*H. duriventris*, *H. dissidens*, *H. punctata*, *H. rondoni*,
156 *H. villasboas*, and *Harttia* sp. 3); and Clade III contained species distributed across
157 Southeastern and South Atlantic drainages and from the La Plata basin (*H. carvalhoi*,
158 *H. torrenticola*, *H. intermontana*, *H. longipinna*, *H. gracilis*, *H. loricariformis*, *H. kronei*,
159 and *Harttia* sp. 1) (**Figure 2a**). The divergence between *Harttia* and *Farlowella* was
160 estimated at ~29.5 million years ago (Mya), with Clade I split about 10 Mya and the
161 divergence between Clades II and III taking place at ~7.9 Mya. The origin of multiple
162 sex chromosome systems was inferred at 5.8 Mya for Clade II (X_1X_2Y system, based
163 on the splitting of *H. punctata*) and at 1.3 Mya for Clade III (XY_1Y_2 system, based on
164 the splitting of *H. intermontana*). The Principal Component Analysis (PCA) of
165 autosomal SNPs (PC1 = 28.5%, PC2 = 18.9%) identified five distinct clusters aligned
166 with phylogenetic clades and geographic distributions **(Supplementary Figure 2)**,
167 categorizing *Harttia* species into three primary clusters, while *Harttia* sp. 2 and the
168 outgroup *Farlowella* sp. constituted separate groups. The complete phylogeny with all

169 individuals is presented in **Supplementary Figure 1**, and complete mean time-
170 calibration estimates are provided in **Supplementary Table 2**.

171 Examining the number of lineages over time reveals two significant shifts
172 (Figure 2b, arrows). These shifts overlap with splitting times that are mostly related to
173 clades with the presence of multiple sex chromosomes, at 2.5 Mya and 1.3 Mya (i.e.,
174 the first for the clade composed of *Harttia* sp. 3, *H. duriventris*, *H. rondoni* and *H.*
175 *villasboas*, and the second for the clade *H. intermontana*, *H. torrenticola, H. carvalhoi*,
176 and *Harttia* sp. 1 (**Figure 2a,b**). Indeed, state-dependent diversification analyses with
177 the Binary State Speciation and Extinction model (BiSSE) revealed substantial
178 differences in speciation rates associated with the presence or absence of multiple sex
179 chromosomes. Lineages with simple sex chromosomes (state 0) exhibited a markedly
180 lower speciation rate (λ_0 = 0.032, CI95% = 0.026-0.290) than those with multiple sex
181 chromosomes (state 1; λ_1 = 0.941, CI95% = 0.485-3.064). The turnover rate for state
182 0 (ε = 1.040, CI95% = 0.776-1.230), calculated as the ratio between extinction and
183 speciation, suggests that extinction is approximately equal to speciation in this group.
184 Additionally, the estimated transition rate ($q_{0\leftrightarrow 1}$) from the absence to the presence of
185 multiple sex chromosomes indicates a moderate probability of trait evolution over time
186 (0.375, CI95% = 0.202-1.530). These modeling results suggest a strong association
187 between the presence of multiple sex chromosomes and increased diversification rates
188 in *Harttia* (p-value = 0.005) (**Figure 2c, Table 1**).

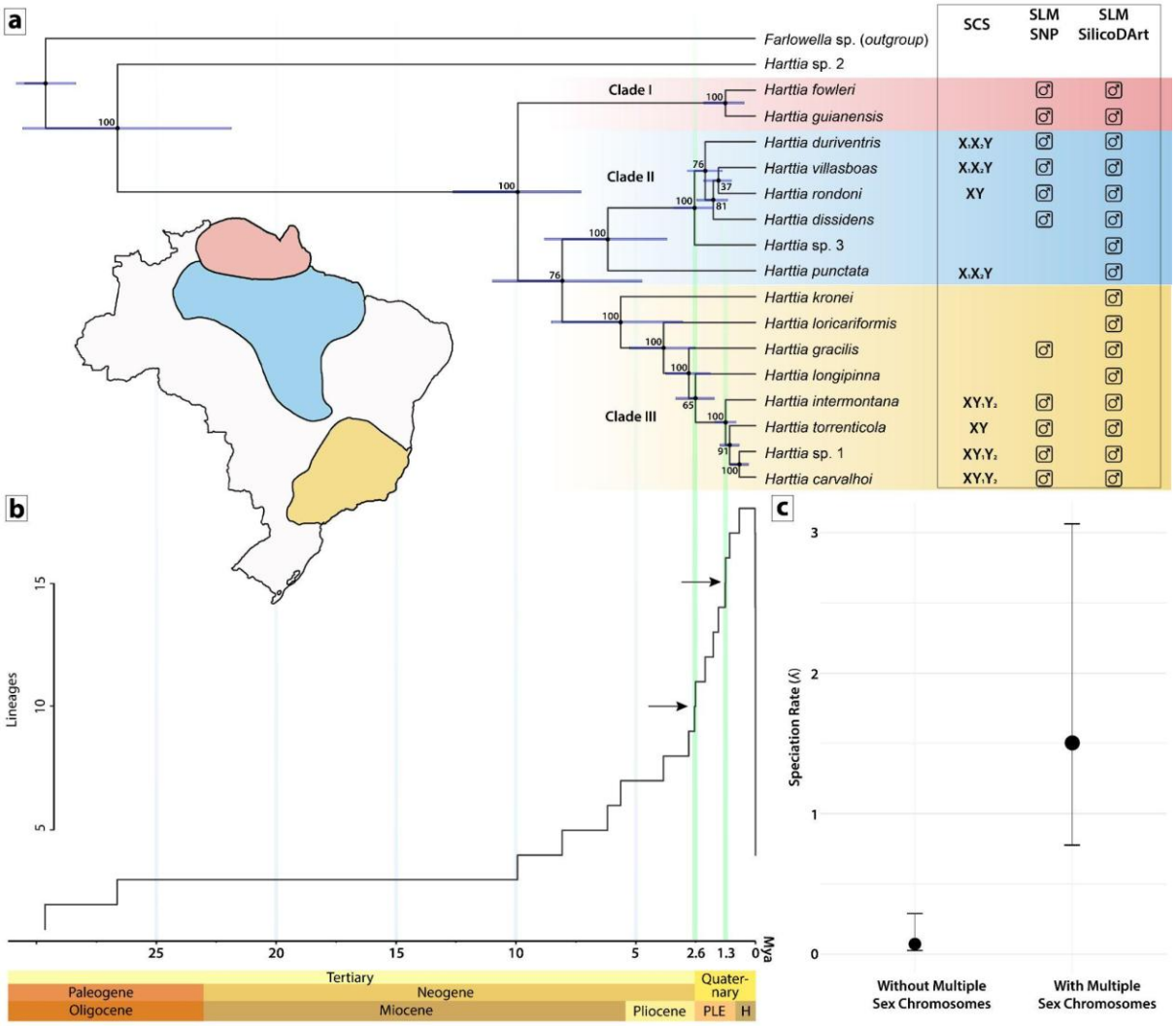

Figure 2. **Evolutionary relationships in *Harttia*. a)** Time-calibrated maximum likelihood phylogenetic relationships of *Harttia* species, using *Farlowella* sp. as an outgroup, recovered from 1,381 autosomal SNPs per species (24,858 SNP markers in total) generated by DArTSeq from 108 individuals. Clade colors correspond to their distribution indicated in the map. Cytogenetically described sex chromosome systems are indicated (SCS). Sex-linked markers, either SNPs or SilicoDArT are presented using the male symbol to indicate male-heterogamety (XY). Node bars correspond to the 95% HPD interval of divergence times and values at nodes indicate bootstrap support. **b)** Lineage through time plot, with arrows indicating major shifts in the number of lineages at 2.6 and 1.3 Mya, accompanied by green lines indicating their coincidence with the rapid diversification of clades with multiple sex chromosomes in the phylogeny. Time scale is the same for both the phylogeny and the lineage through time plot. PLE stands for Pleistocene and H for Holocene. **c)** Speciation rates in clades without and with multiple sex chromosomes inferred by BiSSE. The dots represent the main estimation, and the lines are the 95% confidence intervals.

206 **Table 1.** Parameter estimates from the BiSSE model evaluating the association
207 between the presence of multiple sex chromosomes and diversification rates.
208 Speciation rates (λ) are reported separately for lineages without (state 0) and with
209 (state 1) multiple sex chromosomes. Turnover rate (ε) corresponds to the
210 extinction/speciation ratio for state 0. The transition rate ($q_{0\rightarrow 1}$) reflects the rate of
211 evolution from the absence to the presence of multiple sex chromosomes. Estimates
212 are presented alongside their 95% confidence intervals.

Parameter	Estimate	95% CI
Speciation in clades without multiple sex chromosomes (λ_0)	0.032	0.016 – 0.141
Speciation in clades with multiple sex chromosomes (λ_0)	0.941	0.485 – 1.947
Turnover (ε_0)	1.040	0.858 – 1.243
Transition rate ($q_{0\rightarrow 1}$)	0.248	0.135 – 0.811

213

214 ***2.2 Sex-linked markers***

215 The application of a Bonferroni correction for multiple testing across the 95,305
216 SNP markers generated from the sequencing plate resulted in a stringent per-test
217 significance threshold (P_corrected ≈ 2.62×10^{-6}). This low threshold indicates that
218 the identified sex-linked SNPs are highly unlikely to be false positives arising from
219 random assortment. We focused the false discovery rate calculation on the SNP data
220 due to its co-dominant nature, which provides higher confidence in genotyping calls for
221 assessing sex-linked patterns rather than dominant SilicoDArT markers. Nevertheless,
222 we acknowledge the intrinsic limitations of our sample size (n=3 per sex) and recognize
223 that a greater sampling is required to provide better statistical confidence for the SLM.

224 Across all samples, we identified 443 candidates of sex-linked markers: 95 XY
225 and 16 ZW markers from the SNPs dataset and 316 XY and 16 ZW markers from the
226 SilicoDArT dataset (**Figure 3a; Supplementary Data 1 and 2**). PCA of the sex-linked
227 SNPs (**Supplementary Figure 2**) revealed three main clusters: one composed solely

228 of *H. intermontana*, a second grouping *H. carvalhoi*, *Harttia* sp. 1, and *H. torrenticola*,
229 and a third containing the remaining species, with a minor subcluster of *H. gracilis*.
230 Using a 100% similarity threshold, we identified three shared sex-linked SNPs and 33
231 shared SilicoDArT markers (**Supplementary Table 3**). Shared sex-linked markers
232 were detected in two groups: i) *H. carvalhoi* and *H. intermontana* (XY_1Y_2 system) and
233 ii) a subset of species within Clade II, all in both groups corresponding to XY SLM.
234 Those shared SLMs were only identified inside the groups and not between them,
235 suggesting independent origins of those systems. As an additional step to verify the
236 trustability of the sex-linked markers, since *Harttia* species lack assembled genomes,
237 we cross-mapped the herein obtained SLM in the single Loricariidae chromosome-
238 level genome available at NCBI (*Pterygoplichthys pardalis* ASM5023128v1). Although
239 this genome lacks an identification of sex chromosomes (Lv et al., 2025), we obtained
240 large homologous clusters in chromosomes 2 and 3, suggesting that those SLMs might
241 be not only valid for *Harttia* but also for other loricariids (**Figure 3b**).
242
243

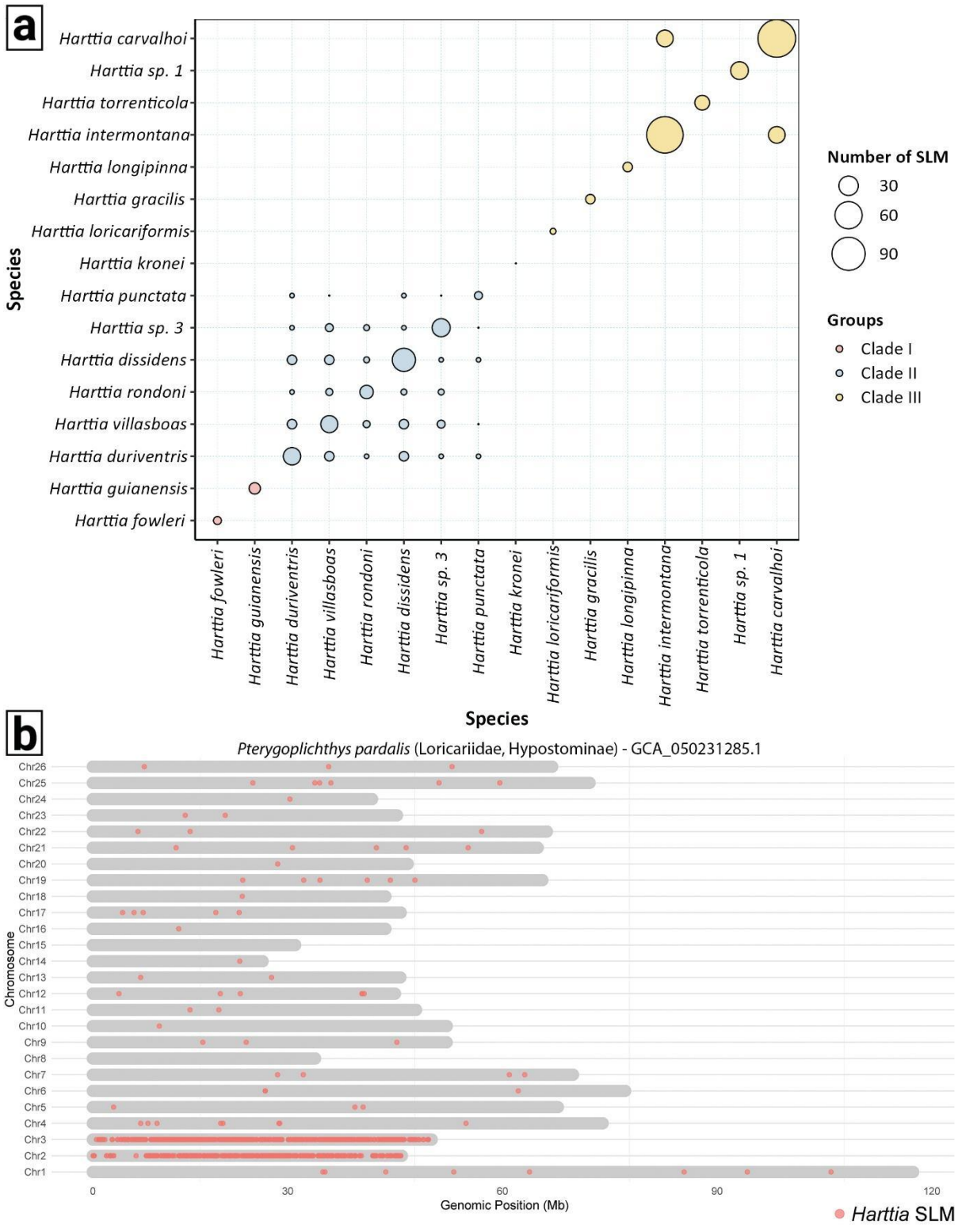

Figure 3. **Summary of sex-linked markers in *Harttia*. a)** Bubble plot showing the number of sex-linked markers per species, colored according to the clade they belong to, as shown in Figure 2. The off-diagonal bubbles represent overlapped sex-linked markers, with the size of the bubble representing the number of these shared SLMs. **b)** Cross-mapping of *Harttia* sex-linked markers in the chromosome-level genome of *Pterygoplichthys pardalis* (Loricariidae, Hypostominae).

251 ***2.3 Biogeographical modeling and ancestral karyotype***

252 A key objective of this study was to infer the historical processes underlying the
253 current distribution and diversity of *Harttia*. We therefore employed biogeographical
254 modeling to estimate ancestral ranges and identify potential dispersal routes, coupled
255 with ancestral chromosome number reconstruction to trace the role of chromosome
256 evolution in speciation. Resolving these questions is fundamental to testing
257 hypotheses about the drivers of diversity in this widely distributed genus. The
258 DIVALIKE model was selected as the best-fitting model based on AICc scores (**Table**
259 **2, Figure 4a**). Although likelihood scores between the DEC and DIVALIKE models
260 showed minimal variation, the estimated ancestral ranges diverged notably after the
261 23 Mya time slice (see **Supplementary Figure 3** for DEC estimates). ΔAIC values
262 indicated only a marginal improvement for DIVALIKE over DEC, the same occurring
263 for Akaike weights (W_i), indicating a little uncertainty between them. Both models
264 converged on similar ancestral area reconstructions after the 10 Mya threshold. The
265 most inclusive *Harttia* clade was inferred to have occupied either the Southern or
266 Southeastern Atlantic drainages (A). The most recent common ancestor of Clade III
267 was likely restricted to the "A", whereas Clade II appears to have been confined to the
268 Amazon Brazilian Shield (B). DIVALike suggested an ancestral distribution along the
269 "A" for the whole *Harttia* clade, with the ancestor of *Harttia* and *Farlowella* likely ranging
270 either on the "A" or "B".

271

272

273

274

275

276 **Table 2.** Models implemented in BioGeoBEARS with their respective Log-likelihood
277 (lnL), dispersal (d), and extinction (e) parameters, corrected Akaike information
278 criterion (AICc), difference in AICc values compared to the best-fit model (ΔAIC), and
279 Akaike weights (W_i).

Model	lnL	*d*	*e*	AICc	ΔAIC	Weight (W_i)
DEC	-39.28528	0.0268696	0.0304716	82.59056	0.97624	0.38
DIVALike	-38.80716	0.02924266	0.02305116	81.61432	0	0.62
BayAreaLike	-45.32449	0.03725671	0.08521665	94.64898	13.03466	0.0009

280

281 The ancestral 2n found at the root of the phylogeny proposed by the model Dys
282 was 2n = 62, indicating that events of descending dysploidy (chromosome fusions)
283 were predominant throughout *Harttia* chromosomal evolution. For the *Harttia* clade
284 (excluding *Farlowella*), the same ancestral 2n was found. In clade III, the ancestral
285 diploid number for species exhibiting cytogenetically identifiable sex chromosomes (*H.*
286 *intermontana*, *H. torrenticola*, *H. carvalhoi*, and *Harttia* sp. 1) is 2n = 56, while in clade
287 II (the most comprehensive clade, including *H. punctata*, *H. duriventris,* and *H.*
288 *villasboas*), it is 2n = 58 (**Figure 4b, Supplementary Data 3**).

289
290
291
292
293
294
295
296
297

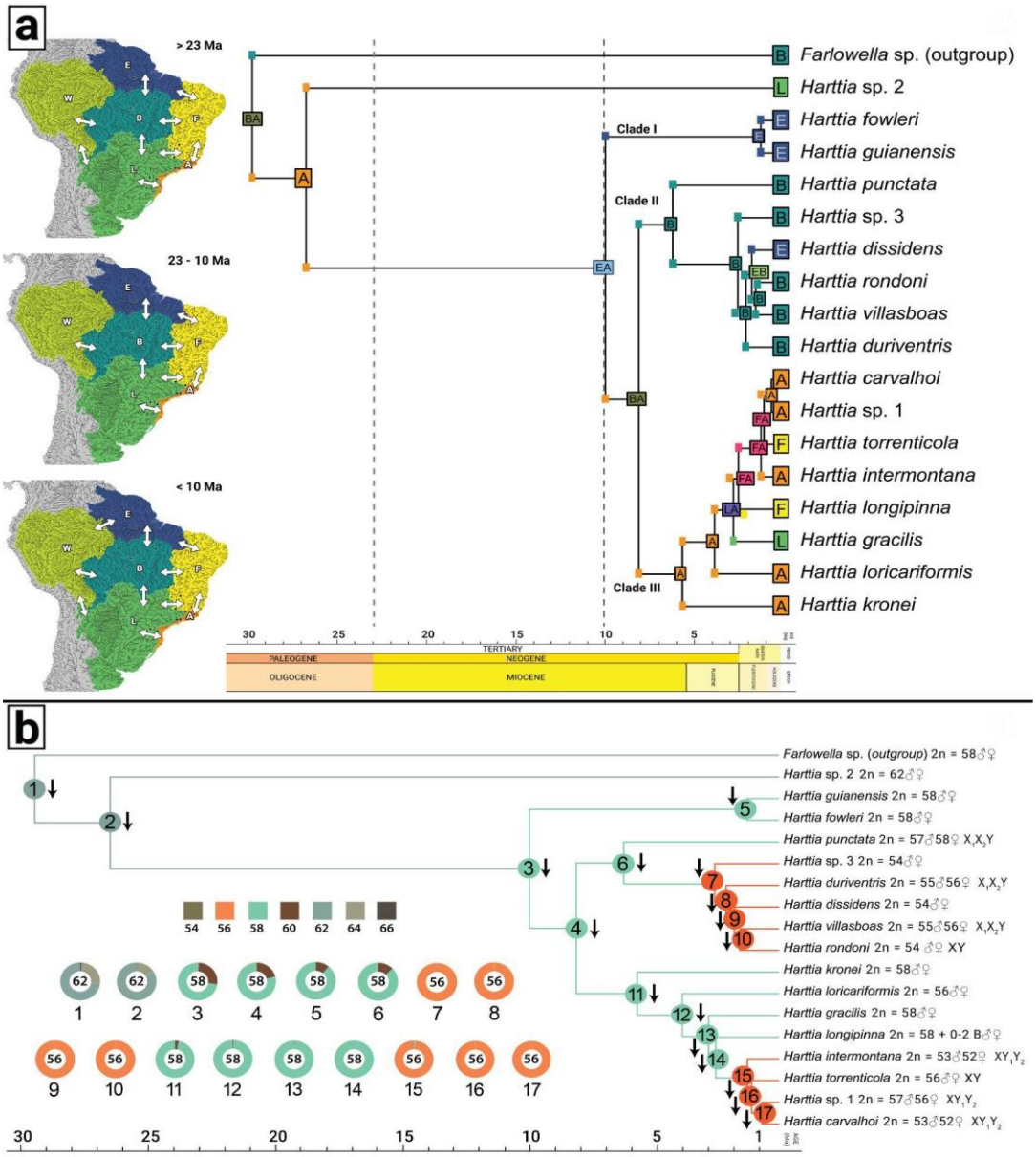

Figure 4. Biogeographic and karyotype modeling for the ancestral characters of *Harttia*. a) Ancestral range of *Harttia* estimated from the best model DIVALike in BioGeoBEARS. Dashed lines correspond to the three time slices defined for modeling: > 23 Mya, 23-10 Mya, and < 10 Mya, which are also represented in the maps with the connections allowed at each (white arrows). The color and letters of tips in phylogeny correspond to the same color in the map on the left, representing the biogeographical areas. At the nodes, the letters represent the sum of the areas of the tips, colored by a mean color of those. **b)** The evolution of diploid numbers in *Harttia* was inferred in ChromEvol v2.0 with the Dys model. Each branch is colored with the same color indicated in the legend for its respective ancestral 2n. Pie charts indicate the probability of the ancestral 2n recovered for each node, indicated by numbers (1-17) in the nodes of the phylogenetic tree. The diploid number and sex chromosome system of the species are shown after their names. Chromosome loss events (down arrows) were predominant (**Supplementary Data 3**).

313 **3. Discussion**

314 Our study suggests that the diversification of *Harttia* is likely driven by a
315 combination of biogeographical events, karyotype restructuring, and multiple
316 independent origins of sex chromosome systems. Our phylogenetic reconstruction
317 suggests that *Harttia* diversification occurred primarily over the past 10 million years,
318 coinciding with major geological and hydrological changes in South America. Notably,
319 the emergence of multiple sex chromosome systems occurred during ~5.6 and ~1.2
320 Mya are associated with accelerated speciation rates, as indicated by BiSSE modeling,
321 suggesting an important role of those systems in the evolution and speciation of the
322 genus. These findings reshape our understanding of the genus and present *Harttia* as
323 a model for studying rapid and recurrent sex chromosome turnover and its role in
324 speciation.

325 The nuclear-based phylogeny based on 1,381 SNPs per species (24,858 SNP
326 markers in total) resolves three major *Harttia* clades but differs from previous
327 mitochondrial and morphological studies. While broadly consistent with earlier studies
328 (Covain et al., 2016; Londoño-Burbano & Reis, 2021), our topology reveals key
329 discrepancies such as the placement of *H. fowleri* within clade I instead of clade II. The
330 distribution of *H. fowleri* (GBIF, 2025) suggests a complex pattern with most registers
331 from Mahury River (French Guyana) and few in drainages from the left bank of the
332 Amazon River in Brazil (e.g. Maicuru River - our sampling site). This region in North
333 Brazil harbors rivers that drain from the Guiana Shield and is a recognized region with
334 poor knowledge on the ichthyofauna (Dagosta and Pinna, 2017, 2019; Dutra et al.,
335 2020). A similar pattern of distribution also occur for the species *H. guianensis* (GBIF,
336 2025), which is also placed in the clade I. Notably, *Harttia* species are usually restricted
337 to small stretches of rivers with rocky or sandy-bottom and fast flowing waters (Rapp

338 Py-Daniel and Oliveira, 2001) and the Amazon River might serve as a great
339 biogeographical barrier for species for clade I and II + III (**Figure 2**), as widely
340 recognized for several terrestrial and aquatic species (Gascon et al., 2000; Pomara et
341 al., 2014; Godinho and Silva, 2018; Pirani et al., 2019;).

342 A distinct sister-group relationship involving *H. dissidens*, indicating more
343 complex interspecific relationships than previously recognized. In our phylogeny, *H.*
344 *dissidens* is sister to the *H. rondoni* + *H. villasboas* clade, with this group forming a
345 sister lineage to the *H. duriventris*, and all these species sister to *H. punctata*, the
346 earliest diverging species in clade II at ~6 mya. In contrast, Londoño-Burbano and Reis
347 (2021) recovered *H. dissidens* as more ancestral to the whole clade II, while in Covain
348 et al. (2016), *H. dissidens* was placed as a sister to most species, with only *H. punctata*
349 showing an older diversification. Besides, *Harttia* sp. 2 was recovered herein as deeply
350 divergent from the remaining *Harttia* species, with an estimated split occurring ~25
351 Mya. This lineage exhibits a distinct karyotype, which is highly similar to that reported
352 in *H. absaberi* (Rodrigues, 2010), with 2n = 62 chromosomes and a high number of
353 interstitial telomeric sites (ITS) (Deon et al., 2020). SLMs are found in all *Harttia*
354 species but *Harttia* sp. 2, supporting a distinction of the latter from the remaining *Harttia*
355 species (**Figure 3**). Indeed, *H. absaberi* was included in the molecular and
356 morphological phylogeny presented by Cherobim (2021), who recovered it as more
357 closely related to other Loricariinae genera than to *Harttia*, suggesting it may warrant
358 placement in a separate genus. Although our sampling included only a single outgroup
359 (*Farlowella*), which diverged from *Harttia* ~30 Mya, the combined evidence from
360 phylogenetic distance, divergence time, and cytogenetic data therefore supports the
361 hypothesis that *Harttia* sp. 2, like *H. absaberi*, may not belong to *Harttia* sensu stricto.

362 Biogeographically, *Harttia* diversification mirrors Neotropical River evolution
363 (**Figure 4a**). The divergence of major clades aligns with the Miocene uplift of the Andes
364 Mountain range that led to the reconfiguration of most drainage systems in South
365 America, especially in the Amazonian region. The distribution of clade II species across
366 formerly interconnected basins (e.g., Tocantins-Araguaia, Xingu, Tapajós) reflects
367 historical dispersal followed by vicariant speciation, a pattern corroborated by similar
368 trends in other loricariid taxa and the highly similar ichthyofauna of those basins, as
369 reported previously in other lineages such as *Cynolebias* spp., *Centromochlus schultzi*,
370 and several Prochilodontidae (Hubert and Reno, 2006; Rossetti et al., 2007; Lima and
371 Ribeiro, 2011; Albert et al., 2018; Roxo et al., 2019; Dagosta et al., 2020). Indeed, the
372 redirection of river courses occurred in the late Miocene, especially proto-Tapajós,
373 proto-Xingu, and proto-Tocantins-Araguaia (Albert et al., 2018), the development of
374 mega-wetlands, and the formation of interfluves such as the Purus Arch and the Serra
375 do Cachimbo introduced new opportunities for both dispersal and vicariant isolation
376 among freshwater organisms, particularly loricariids (Cassemiro et al., 2023), which
377 agrees with the patterns here observed for *Harttia*. Notably, patterns of
378 biogeographical diversification seen in clade III coincide with the time when the uplift
379 of the Serra do Mar and Serra da Mantiqueira Mountain ranges occurred. These events
380 have isolated certain portions of the La Plata Basin from the Atlantic South and
381 Southeastern Drainages, so as from the São Francisco River Basin (Cassemiro et al.,
382 2023, 2025), leading to vicariant processes among their similar ichthyofauna, as also
383 observed for *Salminus* spp. (Machado et al., 2018).
384 Our modeling approaches on both chromosome evolution (ChromEvol) and
385 biogeographical patterns (BioGeoBEARS) support the ancestors of *Harttia* with a
386 distribution in either the Eastern Amazon or Southeast/South Atlantic drainages. The

387 ancestral karyotype was possibly composed of 2n = 58 chromosomes and an XY sex
388 chromosome system, likely in early stages of differentiation (**Figure 5**). Findings thus
389 corroborate earlier hypotheses based on comparative cytogenetics that proposed the
390 same 2n as the ancestral state (Blanco et al., 2017; Deon et al., 2020), therefore,
391 confirming the independent reductions of karyotypes from 2n = 58 to 2n = 56 in *H.*
392 *loricariformis*, *H. villasboas*, and *H. duriventris*, and subsequent reductions of 2n = 54
393 in *H. rondoni* and *Harttia* sp. 3 (Deon et al., 2022a; Sassi et al., 2023a). These
394 karyotype reductions were mostly facilitated by centric fusions, as indicated by our
395 ChromEvol inference (**Figure 4b, Supplementary Data 3**). Nevertheless, these
396 chromosome rearrangements did not involve chromosomal components associated
397 with the intricate multiple sex chromosome systems outlined in the genus (Deon et al.,
398 2022b; Sassi et al., 2023a). The dissociation of autosomal and sex chromosomes
399 dynamics underscores the intricate interaction of lineage-specific and conserved
400 processes, such as Robertsonian translocations and inversions that influence
401 chromosome evolution in this group. Notably, breakpoints in *Harttia* are probably linked
402 to the instability of rDNA loci (Deon et al., 2020, 2022a, b; Sassi et al., 2020, 2023a,
403 b), particularly the 18S rDNA, which is not involved in the creation of the XY_1Y_2.
404 Ribosomal sequences are known to compose evolutionary breakpoint regions among
405 loricariids (e.g., Barros et al., 2017; Glugoski et al., 2018), since they increase genomic
406 instability given the facilitated formation of double-strand breaks by the high
407 transcriptional activity (Berthelot et al., 2015; Warmerdam et al., 2019).
408

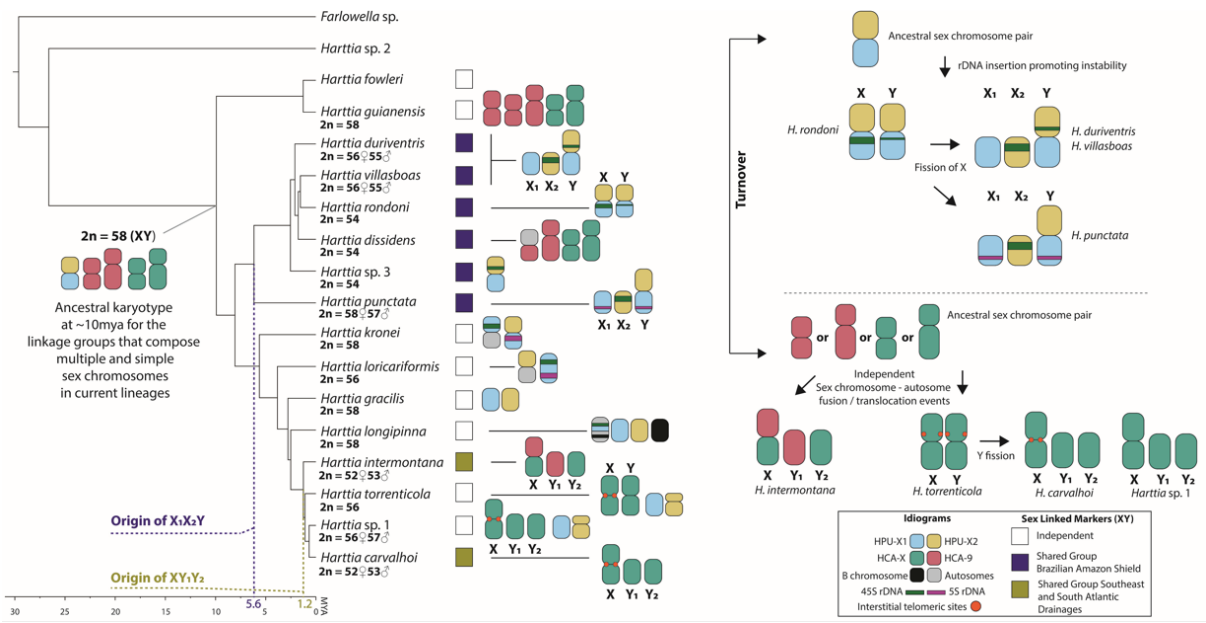

Figure 5. Rapid turnover of multiple sex chromosomes in *Harttia*. A compilation of previous cytogenetic data (Centofante et al., 2006; Blanco et al., 2014, 2017; Deon et al., 2020, 2022a, b, 2024; Sassi et al., 2020, 2021, 2023a, b, 2025) and the results herein obtained with the main hypothesis for the sex chromosome evolution in *Harttia*. Chromosome colors follow the homology patterns established by Deon et al. (2022a, b) and Sassi et al. (2023a, b). Idiograms are presented for each species-specific chromosome, while those pairs not shown in each species tip indicate the conservation of the ancestral state, as depicted on the left. Chromosomes are not drawn to scale.

Our study steer that recurrent turnover and independent evolution of multiple sex chromosomes are probably key mechanisms in the evolution of *Harttia*, reflecting the dynamic nature of sex chromosomes in this group. Across diverse lineages, including plants, fish, and reptiles, recurrent turnover of sex chromosomes within a relatively short evolutionary timescale has been reported (e.g., Keating et al., 2021; Kabir et al., 2022; Wang et al., 2022; Yi et al., 2024; Hayashi et al., 2024; Wang et al., 2024; Zheng et al., 2025), however, none is comparable with *Harttia*, where these events occur within a very short timeframe (~4 My). The arising of multiple sex chromosome systems usually results in postzygotic isolation, mainly due to segregation incompatibilities (White, 1940; Furman et al., 2020; Sember et al., 2021). Rearrangements are also responsible for recombination suppression, which reduces

430 gene flow near rearranged regions (Yannic et al. 2009; McGaugh and Noor 2012;
431 Toups et al. 2019). Furthermore, genes that contribute to reproductive isolation can
432 accumulate on the neo-sex chromosomes, contributing to the speciation process
433 (Kitano et al., 2009; Kitano and Peichel, 2012). We hypothesize that a similar process
434 may have happened on both rearrangement events, which resulted in XY_1Y_2 and X_1X_2Y
435 systems, leading to faster reproductive isolation and speciation. This process was
436 similarly documented in sticklebacks (Kitano et al., 2009; Kitano and Peichel, 2012)
437 and was also proposed for other species such as *Brenthis* butterflies (Mackintosh et
438 al., 2023), African cichlids (Lande et al., 2001; El Taher et al., 2021), and rock wallabies
439 (Potter et al., 2017).

440 Among vertebrates, several mechanisms can drive sex chromosome turnover,
441 including the acquisition of novel sex-determining mutations, translocations of pre-
442 existing sex-determining (SD) genes, chromosomal fusions, and, in some cases,
443 hybridization between populations with distinct SD systems (Kitano and Peichel, 2012;
444 Yoshida and Kitano, 2012; Faber-Hammond et al., 2015; Graves, 2016; Palmer et al.,
445 2019; Bracewell and Bachtrog, 2020; Sember et al., 2021; Bertho et al., 2021; Kabir et
446 al., 2022). Given the absence of sympatric populations of *Harttia*, turnover driven by
447 hybridization events appears unlikely. Instead, the emergence of the XY_1Y_2 system
448 may be best explained by Y-autosome translocation, a mechanism widely reported in
449 teleosts with multiple sex chromosome systems (Sember et al., 2021). In contrast, the
450 X_1X_2Y systems observed in clade II are more consistent with turnovers mediated either
451 by novel SD mutations or translocations of ancestral SD genes. Notably, the
452 association of ribosomal DNA (rDNA) sites with sex chromosomes in species of clade
453 II suggests that rDNA insertions could act as catalysts for recombination suppression
454 by breaking the linkage groups of SD.

455 To validate the presence of sex linked markers, we cross-mapped the herein
456 obtained SLMs to the chromosome-level genome of *Pterygoplichtys pardalis*
457 (divergence from *Harttia* ~36 mya, according to TimeTree5 (Kumar et al., 2017))
458 revealing the large clusterization of those in chromosome pairs 2 and 3 (**Figure 3**).
459 Interestingly, pair 3 of *P. pardalis* results from a fusion of the catfish ancestral
460 microchromosomes 28 and 29 with the ancestral pair 6, carrying genes related to basic
461 cellular metabolism and genomic stability, to signal transduction and transcriptional
462 regulation (Lv et al., 2025). Unfortunately, the study by Lv et al. (2025) do not conduct
463 any approach to investigate putative sex chromosomes in *P. pardalis*, but the
464 clusterization of *Harttia* SLM in two chromosomes suggests that they may represent
465 the two ancestral linkage groups responsible for the origin of the two independently
466 evolved sex chromosomes of *Harttia* (X_1X_2Y and XY_1Y_2). Notably, our PCA analysis of
467 SLM (**Supplementary Figure 2**) do not follow a clear pattern of clusterization related
468 to sex chromosome systems, indicating a big cluster formed by most species and two
469 independent clusters: one formed by *H. carvalhoi*, *H. torrenticola* and *Harttia* sp. 1, and
470 another by *H. intermontana*. This distribution indicates that most *Harttia* species share
471 similarities regarding SLMs and that the XY_1Y_2 has a independent evolutionary pattern,
472 also reinforced by the non-sharing SLMs (**Figure 3**).
473 In conclusion, our study presents the first genome-wide phylogenetic framework
474 for the armored catfish genus *Harttia*, offering new insights into its evolutionary history,
475 chromosomal evolution, and sex chromosome dynamics in teleosts. While broadly
476 congruent with previous hypotheses, our phylogeny reveals several key topological
477 differences, likely attributable to the increased resolution afforded by genome-wide
478 data. Divergence time estimates highlight a relatively recent radiation of *Harttia* sensu
479 stricto over the past 10 million years, tightly associated with major geological and

hydrological transformations in South America driven by the formation of the Amazon River and the rise of the mountain ranges, and potentially accelerated by the rapid turnover of multiple sex chromosomes at 2.6 and 1.3 mya. Our results further support the hypothesis that *Harttia* sp. 2, like *H. absaberi*, falls outside *Harttia* sensu stricto, reflecting deep phylogenetic divergence corroborated by both cytogenetic and molecular evidence, and challenging the monophyly of the genus. Chromosome evolution in *Harttia* is characterized by a dynamic interplay of variation in diploid numbers, lineage-specific reductions via centric fusions, and recurrent turnovers of sex chromosomes, leading to the independent origins of complex multiple sex chromosome systems, which seem crucial in establishing the diversity of the genus. Notably, the integration of sex-linked marker analysis suggests that the evolution of sex chromosomes in *Harttia* is followed not only by structural rearrangements but also by the recruitment of genes associated with reproductive and physiological functions. Together, these findings underscore the potential contribution of multiple sex chromosome systems and their turnovers in accelerating speciation rates when compared to the simple chromosome system representatives. It also reveals the intricate evolutionary processes shaping both genome structure and diversification in Neotropical fishes. Future studies incorporating broader taxonomic and genomic sampling will be essential to further refine the evolutionary history of *Harttia*, a remarkable repository of multiple sex chromosome systems.

502 ## 4. Materials and Methods

503 ### *4.1 Sampling*

504 We selected all *Harttia* species with available cytogenetic data, following those
505 described in **Supplementary Table 1**. The sex of the individuals was recovered from
506 the morphological investigation of the gonads. Fish were anesthetized and euthanized
507 with Eugenol, as approved by the Ethics Committee on Animal Experimentation of the
508 Universidade Federal de São Carlos (Process number CEUA 7994170423).

509

510 ### *4.2 DArTseq and sex-linked markers*

511 Liver tissue samples were collected from six individuals of each species (three
512 males and three females), comprising a full dataset of 107 individuals, and submitted
513 to Diversity Arrays Technology (DArT) Pty Ltd (University of Canberra, Canberra,
514 Australia) for genotyping by sequencing. Briefly, DNA samples were digested with the
515 restriction enzymes *PstI* and *SphI*, followed by adapter ligation and 30 cycles of PCR
516 amplification. Amplified products were sequenced using single end reads on an
517 Illumina HiSeq2000 platform. Data filtering and quality control were performed by DArT
518 Pty Ltd, excluding loci with reproducibility <90% and read depths <3.5× for SNPs and
519 <5× for Silico-DArT markers. For the characterization of sex-linked markers, both
520 SNPs and Silico-DArT loci with missing data were not included in the analysis. For all
521 remaining analyses (PCA, phylogenetic inference), loci with high frequencies of null
522 alleles (call rate <0.85) were filtered out.

523 Candidate sex-linked markers were identified following the pipeline proposed by
524 Lambert et al. (2016). DArTseq datasets were first organized per species and sex,
525 grouping males and females separately. For each individual, SNPs were tallied by
526 heterozygous genotypes (coded as "2") for each sex, using counts of homozygous

genotypes (either "0" for the reference or "1" for the alternate allele) as the baseline. Given that, sex-linked SNPs were defined as SNPs with all individuals from one sex presenting heterozygous genotypes and all individuals from the other sex with homozygous genotypes. On the other hand, sex linked markers from Silico-DArT data (presence and absence) corresponded to those with the presence of the restriction recognition sites in all individuals from one sex but not the other.

The theoretical per-species probability (P) of a SNP randomly assorting by sex purely by chance is calculated as $P = 2^{(1-n)}$ (Lambert et al., 2016), where n is the number of individuals of the minority sex (here, n=3 for all species). This gives $P = 2^{(1-3)} = 0.25$. However, the DArTseq™ protocol optimizes complexity-reduction chemistry at the sequencing plate level, meaning the same genomic regions are interrogated for all samples on a plate. It selects a representative portion of the dataset to verify which restriction enzymes better outcome a complexity reduction for the whole species dataset. Considering that our SNP dataset comprised a total of 95,305 high-confidence markers derived from the same plate chemistry, we used a method to create a conservative genome-wide estimate of the false discovery rate by applying a Bonferroni correction for multiple testing across this entire SNP dataset (N = 95,305). The corrected per-test significance threshold was calculated as: P_corrected = P/N = $0.25/95{,}305 \approx 2.62 \times 10^{-6}$. This extremely stringent threshold means that any SNP exhibiting fixed sex-associated differentiation in a species is highly unlikely to be a false positive. Seeking to validate the SLM herein obtained, we also annotated the SLMs into the only chromosome-level available genome of Loricariidae – *Pterygoplichthys pardalis* (ASM5023128v1) using the 'Annotate from Reference' function from Geneious (Geneious Prime v2025.1, Dotmatics, Boston, USA) with a minimum similarity threshold of 95%. The resulting annotation files for each

552 chromosome (Chr1-26.csv), which included genomic coordinates and feature types,
553 were exported. Subsequent data processing and visualization were conducted in R
554 version 4.3.1, with a custom ggplot2 visualization to plot the distribution of these
555 markers and depicting chromosomes as ideograms (grey horizontal bars) with
556 individual sex-linked markers overlaid as points.

557 To assess potential homology among sex-linked markers, multiple sequence
558 alignments were performed in Geneious (Geneious Prime v2025.1, Dotmatics, Boston,
559 USA) using the MUSCLE algorithm with default settings. Pairs of sequences exhibiting
560 100% similarity were identified from the pairwise distance matrix using a custom R
561 script.

562

563 ***4.3 Time-calibrated phylogeny and Principal Component Analysis***

564 We inferred the evolutionary history of *Harttia* species by Maximum Likelihood
565 using RAxML-ng (Stamatakis, 2014). After filtering out SNPs under selection (5
566 sequences) using Bayescan (Foll and Gaggiotti, 2008), a total of 1,381 SNPs of 107
567 individuals from 18 species (17 *Harttia* + 1 *Farlowella*) were included in the analysis,
568 totalizing 24,858 markers. First, model selection was conducted in ModelTest-NG with
569 seed number defined as “12345”, and all models supported by RAxML-ng were tested
570 (Darriba et al., 2020). ModelTest-NG indicated HKY+I+G4 as the model with the
571 smallest AIC (lnL -118802.5778) and HKY+I as the model with the lowest BIC (lnL
572 240039.7218). The analysis was conducted with 50 initial maximum parsimony trees
573 and 50 initial random trees. The analysis was performed with a total of 1000 bootstraps
574 and mapped into the best tree. The tree with the highest log likelihood was used for
575 time calibration. Finally, the tree was rooted using FigTree v.1.4.4 (Rambaut, 2018),
576 defining *Farlowella* sp. as the outgroup.

577 Coalescent divergence times and population sizes were estimated under the
578 Multispecies Coalescent Model using BPP (Yang, 2015) and calibrated to geological
579 time with bppR (Angelis and dos Reis, 2015). BPP is comprehensive software for
580 Bayesian Markov Chain Monte Carlo (MCMC) analysis, widely applied for species
581 delimitation and divergence times estimation (Yang, 2015). We first performed an A00
582 method analysis (no species delimitation and fixed tree topology). To ensure the
583 consistency of the estimations in our dataset (Flouri et al., 2018; Tiley et al., 2020; Ortiz
584 et al., 2021), we performed independent runs with random subsets of different sizes
585 (300, 400, and 500 SNPs), each with triplicates starting at distinct seed numbers. We
586 assumed a mutation rate (μ) of 3×10^{-9} based on the inferred rate of the *Malapterurus*
587 *electricus*, the closest Siluriformes with μ data (Liu et al., 2024). We also adopted a
588 divergence time estimation of 30 mya for *Harttia* and *Farlowella* based on the mean of
589 estimates on TimeTree5 (Kumar et al., 2022). Considering these values, the theta prior
590 was defined as an inverse gamma distribution of 3 0.002, and the tau prior was set as
591 an inverse gamma distribution of 3 0.18. For this analysis, *Farlowella* was defined as
592 the outgroup. Finetune was allowed, chain length was set to 400,000 generations, with
593 a burn-in of 40,000, and sampling frequency was defined as 2. The first 15% of the
594 samples of each run were discarded as burn-in, and each triplicate was concatenated.
595 Effective sample size (ESS) values were checked on Tracer (Rambaut et al., 2018) to
596 ensure that posterior distributions were adequately estimated. The final time
597 calibrations were defined as the mean of the triplicate outputs with 95% HPD in bppR
598 (**Supplementary Table 2**). We performed a time calibration using a prior node age,
599 based on the mean divergence time of *Harttia* and *Farlowella* estimated on TimeTree5
600 (Kumar et al., 2022). To describe the temporal patterns of cladogenesis within the

genus, we created a lineage-through-time plot (LTT plot) using ape 5.8 (Paradis and Schliep, 2019) on R (R Core Team, 2025).

Principal component analysis (PCA) was conducted using the R package dartR (Gruber et al., 2018; Mijangos et al., 2022). Two distinct datasets were defined, one containing all sex-linked SNPs and a second using the whole SNP dataset, excluding the sex-linked ones (here defined as autosomal SNPs). The most representative PCs were selected for the plot, and the figure was constructed in Adobe Illustrator (Adobe Corporation).

4.4 Character state-dependent branching

We applied the Binary State Speciation and Extinction (BiSSE) model (Maddison et al., 2007) in R (4.3.1) with the package “hisse” (Beaulieu & O’Meara, 2016) to test whether the presence of multiple sex chromosomes is associated with differences in diversification rates. The binary dataset for the character “multiple sex chromosomes” was defined with two states: absence = 0 and presence = 1. We followed the strategy proposed in Lambert et al. (2023), to estimate state-specific speciation rates (λ_0 and λ_1), a single turnover rate ($\varepsilon = \mu/\lambda$) applied to both states, and a single transition rate ($q_{0\leftrightarrow 1}$) between trait states. Likelihood optimization employed an initial simulated annealing phase followed by refinement using a subplex routine to obtain maximum likelihood estimates for speciation rates (λ_0, λ_1), a common turnover rate (ε), and transition rate ($q_{0\leftrightarrow 1}$). Confidence intervals for parameter estimates were derived through likelihood profiling via the SupportRegionHiSSE function, sampling 1000 points within the likelihood support region. To assess whether differences in speciation rates between trait states were statistically significant, we performed a likelihood ratio test (LRT). This involved comparing a full model where speciation rates

626 were allowed to vary between states ($\lambda_0 \neq \lambda_1$) to a constrained null model in which
627 speciation rates were set equal across states ($\lambda_0 = \lambda_1$). The test statistics were
628 calculated as twice the difference in log-likelihoods between the models, which was
629 compared to a chi-squared distribution with one degree of freedom, revealing a p-value
630 of 0.005559656.
631
632 ***4.5 Chromosome number evolution***
633 Chromosome counts and a time-calibrated phylogenetic tree with branch
634 lengths were analyzed in ChromEvol v2.0 (Glick and Mayrose, 2014) to infer ancestral
635 chromosome numbers. We evaluated six default models incorporating ascending
636 dysploidy (single chromosome gains) and descending dysploidy (single chromosome
637 losses) under a time-homogeneous framework. Model adequacy was assessed based
638 on the best-fitting model (Dys). The minimum chromosome number was set to n = 26,
639 corresponding to the lowest value observed in both *Harttia carvalhoi* and *H.*
640 *intermontana*. The maximum chromosome number was set to n = 31, based on the
641 highest diploid count (2n = 62) recorded for *H. absaberi* and *Harttia* sp. 2, the latter
642 included in our dataset.
643
644 ***4.6 Ancestral range estimation***
645 The ancestral range of species was estimated using BioGeoBEARS (Matzke,
646 2018), implemented in R. Three models of range evolution were tested: the dispersal–
647 extinction–cladogenesis (DEC) model (Ree and Smith, 2008), the likelihood version of
648 DIVA - DIVALIKE (Ronquist, 1997), and BAYAREALIKE (Landis et al., 2013). Variants
649 of these models incorporating a founder-event speciation parameter ("j") were not
650 considered, as this parameter has been widely criticized (Ree and Sanmartín, 2018)

651 and is unlikely to accurately represent dispersal in freshwater-restricted taxa where
652 river connectivity is essential for gene flow.

653 Six freshwater ecoregions were defined based on the present-day distribution
654 of species included in the analysis: Western Amazon (W), Eastern Amazon (E),
655 Amazon Brazilian Shield (B), São Francisco and Northeastern drainages (F), Southern
656 and Southeastern Atlantic drainages (A), and the La Plata basin (L). Species
657 distributions were compiled from original descriptions and related literature (Oyakawa
658 et al. 2018) and cross-referenced with occurrence data obtained from GBIF, which
659 were visualized in QGIS (**Supplementary Figure 4**). Given the high endemism of
660 *Harttia* species, which typically do not span multiple regions, we set the maximum
661 number of areas allowed per node to two. This strategy avoids over-constraining the
662 model, as using only a single area per node is not recommended (Matzke, 2018).

663 To account for major historical changes in river connectivity, we defined three
664 time slices based on Neotropical geological history, following frameworks established
665 by Conde-Saldaña et al. (2025): >23 Mya, 23–10 Mya, and <10 Mya. These periods
666 encompass key events in river capture and paleodrainage evolution of the Neotropical
667 region (Albert et al., 2006, 2018, 2021; Tagliacollo et al., 2015; Montes et al., 2021).
668 The map representing these connections was created using QGIS 3.28.2-Firenze
669 using merged ecoregions from Abell et al. (2008).

670

671

672

673

674

675

Data availability statement

All the data and scripts used for this study are available at https://github.com/sassichico/harttia.

Acknowledgements

We appreciate the contributions of Osvaldo Oyakawa, Lúcia Rapp-Py Daniel for the identification of species used in this work, and to Claudio Oliveira, Vladimir Trifonov, José Maurício Barbanti Duarte, Francisco Langeani, and Orlando Moreira Filho for the valuable insights. We also thank Eliana Feldberg and all members of Laboratório de Genética Animal - INPA, so as Marcelo Vicari, Luiz Henrique Silva, and Antonio Donizete, for the assistance in collecting specimens.

Study Funding

FMCS is funded by Conselho Nacional de Desenvolvimento Científico e Tecnológico (PDE-CNPq 200247/2025-5) and was supported during part this study by FAPESP 2020/02681-9, 2022/04261-2, and 2023/08116-0. MBC was supported by FAPESP (2023/00955-2).

References

1. Abell R, Thieme ML, Revenga C, Bryer M, Kottelat M, Bogutskaya N, Coad B, Mandrak N, Balderas SC, Bussing W, et al. 2008. Freshwater Ecoregions of the World: A New Map of Biogeographic Units for Freshwater Biodiversity Conservation. *Bioscience* 58:403-414.
2. Alam SMI, Prasongmaneerut T, Gleeson D, Georges A, Sarre SD, Srikulnath K, Ezaz T. 2018. Sex-Determination mechanisms among populations within

701 cryptic species complex of *Calotes* (Squamata: Agamidae: Draconinae). *DNA*
702 1:49-67.
703 3. Albert JS, Lovejoy NR, Crampton WGR. 2006. Miocene tectonism and the
704 separation of cis- and trans-Andean river basins: Evidence from Neotropical
705 fishes. *J South Am Earth Sci.* 21:14-27.
706 4. Albert JS, Val P, Hoorn C. 2018. The changing course of the Amazon River in
707 the Neogene: center stage for Neotropical diversification. *Neotrop Ichthyol.* 16:
708 e180033.
709 5. Albert JS, Bernt MJ, Fronk AH, Fontenelle JP, Kuznar SL, Lovejoy NR. 2021.
710 Late Neogene megariver captures and the Great Amazonian biotic interchange.
711 *Glob Planet Change*. 205:103554.
712 6. Angelis K, Dos Reis M. 2015. The impact of ancestral population size and
713 incomplete lineage sorting on Bayesian estimation of species divergence times.
714 *Curr Zool.* 61:874-885.
715 7. Aznar-Fernández T, Barilli E, Cobos MJ, Kilian A, Carling J, Rubiales D. 2020.
716 Identification of quantitative trait loci (QTL) controlling resistance to pea weevil
717 (*Bruchus pisorum*) in a high-density integrated DArTseq SNP-based genetic
718 map of pea. *Sci Rep*. 10:33.
719 8. Baloch FS, Alsaleh A, Shahid MQ, Çiftçi V, Sáenz de Miera LE, Aasim M,
720 Nadeem MA, Aktaş H, Özkan H, Hatipoğlu R. 2017. A whole genome DArTseq
721 and SNP analysis for genetic diversity assessment in durum wheat from central
722 fertile crescent. *PLoS One.* 12:e0167821.
723 9. Barros AV, Wolski MAV, Nogaroto V, Almeida MC, Moreira-Filho O, Vicari MR.
724 2017. Fragile sites, dysfunctional telomere and chromosome fusions: What is
725 5S rDNA role? *Gene*. 608:20-27.

10. Beaulieu JM, O'Meara BC. 2016. Detecting hidden diversification shifts in models of trait-dependent speciation and extinction. *Syst Biol*. 65:583-601.
11. Berthelot C, Muffato M, Abecassis J, Crollius HR. 2015. The 3D organization of chromatin explains evolutionary fragile genomic regions. *Cell Rep*. 10:1913-1924.
12. Bertho S, Herpin A, Schartl M, Guiguen Y. 2021. Lessons from an unusual vertebrate sex-determining gene. *Philos Trans R Soc Lond B Biol Sci*. 376:20200092.
13. Blanco DR, Vicari MR, Lui RL, Artoni RF, Almeida MC, Traldi JB, Margarido VP, Moreira-Filho O. 2014. Origin of the $X_1X_1X_2X_2/X_1X_2Y$ sex chromosome system of *Harttia punctata* (Siluriformes, Loricariidae) inferred from chromosome painting and FISH with ribosomal DNA markers. *Genetica.* 142:119–126.
14. Bracewell R, Bachtrog D. 2020. Complex evolutionary history of the Y chromosome in flies of the *Drosophila obscura* species group. *Genome Biol Evol*. 12:494-505.
15. Cassemiro FAS, Albert JS, Antonelli A, Menegotto A, Wüest RO, Cerezer F, Reis RE, Tan M, Tagliacollo V, et al. 2023. Landscape dynamics and diversification of the megadiverse South American freshwater fish fauna. *Proc Natl Acad Sci U S A*. 120:e2211974120.
16. Cassemiro FAS, Salgado AAR, Paixão RW, Rezende EA. 2025. The timing of large drainage rearrangement in South America: A study based on morphological and ecological evidence. *Geomorphology*. 468:109457.
17. Centofante L, Bertollo LAC, Moreira-Filho O. 2006. Cytogenetic characterization and description of an XX/XY_1Y_2 sex chromosome system in

750 catfish Harttia carvalhoi (Siluriformes, Loricariidae). *Cytogenet Genome Res*.
751 112:320-024.
752 18. Charlesworth D. 2017. Evolution of recombination rates between sex
753 chromosomes. *Philos Trans R Soc Lond B Biol Sci*. 372:20160456.
754 19. Charlesworth D, Charlesworth B. 1980. Sex differences in fitness and selection
755 for centric fusions between sex-chromosomes and autosomes. *Genet Res*,
756 35:205-214.
757 20. Cherobim A, unpublished data,
758 https://repositorio.unesp.br/entities/publication/32eef081-dd13-452f-949b-
759 84968a795e84, last accessed August 08, 2025.
760 21. Conde-Saldaña CC, Melo BF, Roxo FF, Tagliacollo VA, Oliveira C, Albert JS.
761 2025. Landscape Evolution Drives Continental Diversification in Neotropical
762 Freshwater Fishes of the Family Erythrinidae (Teleostei, Characiformes). *J*
763 *Biogeogr*. 52:e15129.
764 22. Conesa A, Götz S, García-Gómez JM, Terol J, Talón M, Robles M. 2005.
765 Blast2GO: a universal tool for annotation, visualization and analysis in functional
766 genomics research. *Bioinformatics* 21:3674-3676.
767 23. Covain R, Fisch-Muller S, Oliveira C, Mol JH, Montoya-Burgos JI, Dray S. 2016.
768 Molecular phylogeny of the highly diversified catfish subfamily Loricariinae
769 (Siluriformes, Loricariidae) reveals incongruences with morphological
770 classification. *Mol Phylogenet Evol*. 94:492-517.
771 24. Dagosta FCP, de Pinna M. 2017. Biogeography of Amazonian fishes:
772 deconstructing river basins as biogeographic units. *Neotrop Ichthyol*. 15:
773 e170034.

774 25. Dagosta FCP, de Pinna M. 2019. The fishes of the Amazon: distribution and
775 biogeographical patterns, with a comprehensive list of species. *Bull Am Mus*
776 *Nat Hist*. 431:1-163.
777 26. Dagosta FCP, de Pinna M, Peres CA, Tagliacollo VA. 2021. Existing protected
778 areas provide a poor safety-net for threatened Amazonian fish species. *Aquat*
779 *Conserv*. 31:1167-1189.
780 27. Darriba D, Posada D, Kozlov AM, Stamatakis A, Morel B, Flouri T. 2020.
781 ModelTest-NG: a new and scalable tool for the selection of DNA and protein
782 evolutionary models. *Mol Biol Evol*. 37:291-294.
783 28. Davey JW, Hohenlohe PA, Etter PD, Boone JQ, Catchen JM, Blaxter ML. 2011.
784 Genome-wide genetic marker discovery and genotyping using next-generation
785 sequencing. *Nat Rev Genet*. 12:499-510.
786 29. Deon GA, Glugoski L, Vicari MR, Nogaroto V, Sassi FMC, Cioffi MB, Liehr T,
787 Bertollo LAC, Moreira-Filho O. 2020. Highly Rearranged Karyotypes and
788 Multiple Sex Chromosome Systems in Armored Catfishes from the Genus
789 *Harttia* (Teleostei, Siluriformes). *Genes*. 11:1366.
790 30. Deon GA, Glugoski L, Hatanaka T, Sassi FMC, Nogaroto V, Bertollo LAC, Liehr
791 T, Al-Rikabi A, Moreira-Filho O, Cioffi MB, Vicari MR. 2022a. Evolutionary
792 breakpoint regions and chromosomal remodeling in *Harttia* (Siluriformes:
793 Loricariidae) species diversification. *Genet Mol Biol.* 45:e20210170.
794 31. Deon GA, Glugoski L, Sassi FMC, Hatanaka T, Nogaroto V, Bertollo LAC, Liehr
795 T, Al-Rikabi A, Moreira-Filho O, Cioffi MB, Vicari MR. 2022b. Chromosomal
796 Rearrangements and Origin of the Multiple XX/XY_1Y_2 Sex Chromosome System
797 in *Harttia* Species (Siluriformes: Loricariidae). *Front Genet*. 13:877522.

32. Deon GA, dos Santos RZ, Sassi FMC, Moreira-Filho O, Vicari MR, Porto-Foresti F, Utsunomia R, Cioffi MB. The role of satellite DNAs in the chromosomal rearrangements and the evolution of the rare XY_1Y_2 sex system in *Harttia* (Siluriformes: Loricariidae). *J Hered*. 115:541-551.
33. Dobry J, Wapstra E, Stringer EJ, Gruber B, Deakin JE, Ezaz T. 2023. Widespread chromosomal rearrangements preceded genetic divergence in a monitor lizard, *Varanus acanthurus* (Varanidae). *Chromosome Res*. 31:9.
34. Dutra GM, Freitas TMS, Prudente BS, Salvador GN, Leão MDV, Peixoto LAW, Mendonça MB, Netto-Ferreira AL, Silva FR, Montag LFA, Wosiacki WB. 2020. Rapid assessment of the ichthyofauna of the southern Guiana Shield tributaries of the Amazonas River in Pará, Brazil. *Acta Amazon.* 50:24-36.
35. El Taher A, Ronco F, Matschiner M, Salzburger W, Böhne A. 2021. Dynamics of sex chromosome evolution in a rapid radiation of cichlid fishes. *Sci Adv*. 7:eabe8215.
36. Faber-Hammond JJ, Phillips RB, Brown KH. 2015. Comparative analysis of the shared sex-determination region (SDR) among salmonid fishes. *Genome Biol Evol.* 7:1972-1987.
37. Flouri T, Jiao X, Rannala B, Yang Z. 2018. Species tree inference with BPP using genomic sequences and the multispecies coalescent. *Mol Biol Evol.* 35:2585-2593.
38. Foll M, Gaggiotti O. 2008. A genome-scan method to identify selected loci appropriate for both dominant and codominant markers: a Bayesian perspective. *Genetics.* 180:977-993.
39. Fricke R, Eschmeyer WN, van der Laan R. 2025. Eschmeyer's Catalog of Fishes: Genera, Species, References. Available at

823 http://researcharchive.calacademy.org/research/ichthyology/catalog/fishcatmain.asp. Last accessed August 02, 2025.
825 40. Furman BL, Metzger DC, Darolti I, Wright AE, Sandkam BA, Almeida P, Shu JJ, Mank JE. 2020. Sex chromosome evolution: so many exceptions to the rules. *Genome Biol Evol*. 12:750-763.
828 41. Gabilondo, A. R., Pérez, L. H., & Rodríguez, R. M. 2021. Hormonal and neuroendocrine control of reproductive function in teleost fish. *Rev Bionat*. 6:2122-2133.
831 42. Gascon C, Malcolm JR, Patton JL, da Silva MNF, Bogart JP, Lougheed SC, Peres CA, Neckel S, Boag PT. 2000. Riverine barriers and the geographic distribution of Amazonian species. *Proc Natl Acad Sci USA*. 97:13672-13677.
834 43. Glick L, Mayrose I. 2014. ChromEvol: assessing the pattern of chromosome number evolution and the inference of polyploidy along a phylogeny. *Mol Biol Evol*. 31:1914-1922.
837 44. Glugoski L, Giuliano-Caetano L, Moreira-Filho O, Vicari MR, Nogaroto V. 2018. Co-located hAT transposable element and 5S rDNA in an interstitial telomeric sequence suggest the formation of Robertsonian fusion in armored catfish. *Gene*. 650:49-54.
841 45. Godinho MBC, Da Silva FR. 2018. The influence of riverine barriers, climate, and topography on the biogeographic regionalization of Amazonian anurans. *Sci Rep*. 8:3427.
844 46. Graves JAM. 2006. Sex chromosome specialization and degeneration in mammals. *Cell*. 124:901-914.
846 47. Graves JAM. 2016. Evolution of vertebrate sex chromosomes and dosage compensation. *Nat Rev Genet.* 17:33-46.

48. Gruber B, Unmack PJ, Berry OF, Georges A. 2018. dartr: An r package to facilitate analysis of SNP data generated from reduced representation genome sequencing. *Mol Ecol Resour.* 18:691-699.
49. Hayashi S, Abe T, Igawa T, Katsura Y, Kazama Y, Nozawa M. 2024. Sex chromosome cycle as a mechanism of stable sex determination. *J Biochem.* 176:81-95.
50. Hospodářská M, Mora P, Voleníková AC, Al-Rikabi A, Altmanová M, Simanovsky SA, Tolar N, Pavlica T, Janečková K, Štundlová J, et al. 2025. Multiple Origins of Sex Chromosomes in *Nothobranchius* Killifishes. *Mol Ecol*. 0:e70029.
51. Hubert N, Renno JF. 2006. Historical biogeography of South American freshwater fishes. *J Biogeogr.* 33:1414-1436.
52. Jaccoud D, Peng K, Feinstein D, Kilian A. 2001. Diversity arrays: a solid state technology for sequence information independent genotyping. *Nucleic Acids Res*. 29:e25.
53. Kabir A, Ieda R, Hosoya S, Fujikawa D, Atsumi K, Tajima S, Nozawa A, Koyama T, Hirase S, Nakamura O, et al. 2022. Repeated translocation of a supergene underlying rapid sex chromosome turnover in *Takifugu* pufferfish. *Proc Natl Acad Sci U S A*. 119:e2121469119.
54. Keating SE, Blumer M, Grismer LL, Lin A, Nielsen SV, Thura MK, Wood PL, Wuah ES, Gamble T. 2021. Sex chromosome turnover in bent-toed geckos (*Cyrtodactylus*). *Genes*. 12:116.
55. Kirschner P, Perez MF, Záveská E, Sanmartín I, Marquer L, Schlick-Steiner BC, Alvarez, the STEPPE Consortium, Steiner FM, Schönswetter P. 2022.

872 Congruent evolutionary responses of European steppe biota to late Quaternary
873 climate change. *Nat Comm*. 13:1921.
874 56. Kitano J, Peichel CL. 2012. Turnover of sex chromosomes and speciation in
875 fishes. *Environ Biol Fishes*. 94:549-558.
876 57. Kitano J, Ross JA, Mori S, Kume M, Jones FC, Chan YF, Absher DM, Grimwood
877 J, Schmutz J, Myers RM, et al. 2009. A role for a neo-sex chromosome in
878 stickleback speciation. *Nature*. 461:1079-1083.
879 58. Knief U, Müller IA, Stryjewski KF, Metzler D, Sorenson M, Wolf JB. 2024.
880 Evolution of chromosomal inversions across an avian radiation. *Mol Biol Evol.*
881 41:msae092.
882 59. Kottler VA, Schartl M. 2018. The colorful sex chromosomes of teleost fish.
883 *Genes*. 9:233.
884 60. Kratochvíl L, Stöck M, Rovatsos M, Bullejos M, Herpin A, Jeffries DL, Peichel
885 CL, Perrin N, Valenzuela N, Pokorná MJ. 2021. Expanding the classical
886 paradigm: what we have learnt from vertebrates about sex chromosome
887 evolution. *Philos Trans R Soc Lond B Biol Sci*. 376:20200097.
888 61. Krysanov E, Demidova T. 2018. Extensive karyotype variability of African fish
889 genus *Nothobranchius* (Cyprinodontiformes). *Comp Cytogenet*. 12:387.
890 62. Kumar S, Suleski M, Craig JM, Kasprowicz AE, Sanderford M, Li M, Stecher G,
891 Hedges SB. 2022. TimeTree 5: an expanded resource for species divergence
892 times. *Mol Biol Evol.* 39:msac174.
893 63. Lambert MR, Skelly DK, Ezaz T. 2016. Sex-linked markers in the North
894 American green frog (*Rana clamitans*) developed using DArTseq provide early
895 insight into sex chromosome evolution. *BMC Genomics*. 17:844.

896 64. Lambert S, Voznica J, Morlon H. 2023. Deep Learning from Phylogenies for
897 Diversification Analyses. *Sys Biol.* 72:1262-1279.
898 65. :Lande R, Seehausen O, van Alphen JJ. 2001. Mechanisms of rapid sympatric
899 speciation by sex reversal and sexual selection in cichlid fish. *Genetica*.
900 112:435-443.
901 66. L-andis MJ, Matzke NJ, Moore BR, Huelsenbeck J. 2013. Bayesian analysis of
902 biogeography when the number of areas is large. *Sys Biol*. 62:789-804.
903 67. Li J, Zhou W, Wang Y, Niu C. 2018. The dual role of cGMP in oocyte maturation
904 of zebrafish. *Biochem Biophys Res Commun*. 499:998-1003.
905 68. Lima FC, Ribeiro AC. 2011. Continental-scale tectonic controls of biogeography
906 and ecology. *Historical biogeography of neotropical freshwater fishes*.
907 University of California Press, Berkeley, 145-164.
908 69. Liu M, Song Y, Zhang S, Yu L, Yuan Z, Yang H, Zhang M, Zhou Z, Seim I, Liu
909 S, et al. 2024. A chromosome-level genome of electric catfish (Malapterurus
910 electricus) provided new insights into order Siluriformes evolution. *Mar Life Sci*
911 *Technol*. 6:1–14
912 70. Londoño-Burbano A, Reis RE. 2021. A combined molecular and morphological
913 phylogeny of the Loricariinae (Siluriformes: Loricariidae), with emphasis on the
914 Harttiini and Farlowellini. *PloS One*. 16:e0247747.
915 71. Machado CB, Galetti Jr PM, Carnaval AC. 2018. Bayesian analyses detect a
916 history of both vicariance and geodispersal in Neotropical freshwater fishes. *J*
917 *Biogeogr*. 45:1313-1325.
918 72. Mackintosh A, Vila R, Laetsch DR, Hayward A, Martin SH, Lohse K. 2023.
919 Chromosome fissions and fusions act as barriers to gene flow between *Brenthis*
920 fritillary butterflies. *Mol Biol Evol.* 40:msad043.

921 73. Maddison WP, Midford PE, Otto SP. 2007. Estimating a binary character's effect
922 on speciation and extinction. *Syst Biol*. 56:701-710.
923 74. Matzke NJ. 2018. BioGeoBEARS: BioGeography with Bayesian (and likelihood)
924 Evolutionary Analysis with R Scripts. version 1.1.1, published on GitHub on
925 November 6, 2018. DOI: http://dx.doi.org/10.5281/zenodo.1478250
926 75. McGaugh SE, Noor MA. 2012. Genomic impacts of chromosomal inversions in
927 parapatric *Drosophila* species. *Philos Trans R Soc Lond B Biol Sci*. 367:422-
928 429.
929 76. Melville J, Haines ML, Boysen K, Hodkinson L, Kilian A, Smith Date KL, Potvin
930 DA, Parris KM. 2017. Identifying hybridization and admixture using SNPs:
931 application of the DArTseq platform in phylogeographic research on
932 vertebrates. *R Soc Open Sci.* 4:161061.
933 77. Mijangos JL, Gruber B, Berry O, Pacioni C, Georges A. 2022. dartR v2: An
934 accessible genetic analysis platform for conservation, ecology and agriculture.
935 *Methods Ecol Evol*. 13:2150-2158.
936 78. Mirarab S, Bayzid MS, Warnow T. 2016. Evaluating summary methods for
937 multilocus species tree estimation in the presence of incomplete lineage sorting.
938 *Sys Biol*. 65:366-380.
939 79. Montes C, Silva CA, Bayona GA, Villamil R, Stiles E, Rodriguez-Corcho AF,
940 Beltrán-Triviño A, Lamus F, Muñoz-Granados MD, Pérez-Angel LC, et al. 2021.
941 A middle to late Miocene trans-Andean portal: Geologic record in the Tatacoa
942 Desert. *Front Earth Sci*. 8:587022.
943 80. Mujyambere V, Adomako K, Olympio OS. 2024. Effectiveness of DArTseq
944 markers application in genetic diversity and population structure of indigenous
945 chickens in Eastern Province of Rwanda. *BMC Genomics*. 25:193.

946 81. Muller HJ. 1918. Genetic variability, twin hybrids and constant hybrids, in a case
947 of balanced lethal factors. *Genetics*. 3:422.
948 82. Nedoluzhko A, Sharko F, Tsygankova S, Boulygina E, Ibragimova A, Teslyuk
949 A, Galindo-Villegas J, Rastorguev S. Genomic evidence supports the
950 introgression between two sympatric stickleback species inhabiting the White
951 Sea basin. *Heliyon*. 7:e06160.
952 83. Ohno S. 1966. Differentiation of the Primitive Sex Elements at the Expense of
953 the Y or W, and the Conservation of the Original X or Z. In Sex Chromosomes
954 and sex-linked genes (13-24). Berlin, Heidelberg: Springer Berlin Heidelberg.
955 84. Ortiz D, Pekár S, Bilat J, Alvarez N. 2021. Poor performance of DNA barcoding
956 and the impact of RAD loci filtering on the species delimitation of an Iberian ant-
957 eating spider. *Mol Phylogenet Evol.* 154:106997.
958 85. Oyakawa O, Fichberg I, Rapp-Py Daniel LH. Three new species of *Harttia*
959 (Loricariidae: Loricariinae) from Serra do Cachimbo, rio Xingu basin, Pará,
960 Northern Brazil. *Zootaxa*. 4387:75–90.
961 86. Palmer DH, Rogers TF, Dean R, Wright AE. 2019. How to identify sex
962 chromosomes and their turnover. *Mol Ecol*. 28:4709-4724.
963 87. Paradis E, Schliep K. 2019. ape 5.0: an environment for modern phylogenetics
964 and evolutionary analyses in R. *Bioinformatics*. 35:526-528.
965 88. Pennell MW, Kirkpatrick M, Otto SP, Vamosi JC, Peichel CL, Valenzuela N,
966 Kitano J. 2015. Y fuse? Sex chromosome fusions in fishes and reptiles. *PLoS*
967 *Genet*. 11:e1005237.
968 89. Pirani RM, Werneck FP, Thomaz AT, Kenney ML, Sturaro MJ, Ávila-Pires TCS,
969 Peloso PLV, Rodrigues MT, Knowles LL. Testing main Amazonian rivers as

970 barriers across time and space within widespread taxa. *J Biogeogr.* 46:2444-
971 2456.
972 90. Pokorná M, Altmanová M, Kratochvíl L. 2014. Multiple sex chromosomes in the
973 light of female meiotic drive in amniote vertebrates. *Chrom Res*. 22:35-44.
974 91. Potter S, Bragg JG, Blom MP, Deakin JE, Kirkpatrick M, Eldridge MD, Moritz C.
975 2017. Chromosomal speciation in the genomics era: disentangling phylogenetic
976 evolution of rock-wallabies. *Front Genet.* 8:10.
977 92. Rambaut A. 2018. FigTree v1. 4.4. Available at
978 https://github.com/rambaut/figtree/releases/tag/v1.4.4.
979 93. Rambaut A, Drummond AJ, Xie D, Baele G, Suchard MA. 2018. Posterior
980 summarization in Bayesian phylogenetics using Tracer 1.7. *Syst Biol*, 67:901-
981 904.
982 94. Rapp Py-Daniel LH. 1997. Unpublished data: Phylogeny of the Neotropical
983 armored catfishes of the subfamily Loricariinae (Siluriformes: Loricariidae).
984 Available at
985 https://www.proquest.com/openview/8b63544fca6e7c4586db5dccff3e4e05/1?
986 pq-origsite=gscholar&cbl=18750&diss=y.
987 95. Ree RH, Smith SA. 2008. Maximum likelihood inference of geographic range
988 evolution by dispersal, local extinction, and cladogenesis. *Syst Biol*. 57:4-14.
989 96. Ree RH, Sanmartín I. 2018. Conceptual and statistical problems with the DEC+
990 J model of founder-event speciation and its comparison with DEC via model
991 selection. *J Biogeogr*. 45:741-749.
992 97. Ronquist F. 1997. Dispersal-vicariance analysis: a new approach to the
993 quantification of historical biogeography. *Syst Biol*, 46:195-203.

994 98. Rossetti DF, Valeriano MM. 2007. Evolution of the lowest amazon basin
995 modeled from the integration of geological and SRTM topographic data. *Catena*.
996 70:253-265.
997 99. Roxo FF, Ochoa LE, Sabaj MH, Lujan NK, Covain R, Silva GSC, Melo BF, Albert
998 JS, Chang J, Foresti F, et al. Phylogenomic reappraisal of the Neotropical
999 catfish family Loricariidae (Teleostei: Siluriformes) using ultraconserved
1000 elements. *Mol Phylogenet Evol*. 135:148-165.
1001 100. Sassi FMC, Deon GA, Moreira-Filho O, Vicari MR, Bertollo LAC, Liehr T,
1002 Oliveira EA, Cioffi MB. 2020. Multiple Sex Chromosomes and Evolutionary
1003 Relationships in Amazonian Catfishes: The Outstanding Model of the Genus
1004 *Harttia* (Siluriformes: Loricariidae). *Genes*. 11:1179.
1005 101. Sassi FMC, Moreira-Filho O, Deon GA, Sember A, Bertollo LAC, Liehr T,
1006 Oliveira VCS, Viana PF, Feldberg E, Vicari MR, Cioffi MB. 2021. Adding New
1007 Pieces to the Puzzle of Karyotype Evolution in *Harttia* (Siluriformes,
1008 Loricariidae): Investigation of Amazonian Species. *Biology*. 10:922.
1009 102. Sassi FMC, Sember A, Deon GA, Liehr T, Padutsch N, Oyakawa OT,
1010 Vicari MR, Bertollo LAC, Moreira-Filho O, Cioffi MB. 2023a. Homeology of sex
1011 chromosomes in Amazonian *Harttia* armored catfishes supports the X-fission
1012 hypothesis for the X_1X_2Y sex chromosome system origin. *Sci Rep.* 13:15756.
1013 103. Sassi FMC, Deon GA, Sember A, Liehr T, Oyakawa OT, Moreira-Filho
1014 O, Bertollo LAC, Vicari MR, Cioffi MB. 2023b. Turnover of multiple sex
1015 chromosomes in Harttia catfish (Siluriformes, Loricariidae): a glimpse from
1016 whole chromosome painting. *Front Genet*. 14:1226222.

1017 104. Sassi FMC, Cioffi MB, Moreira-Filho O. 2024. A state-of- art review of
1018 Loricariidae (Ostariophysi: Siluriformes) cytogenetics. *Neotrop Ichthyol*.
1019 22:e240050.
1020 105. Sassi FMC, Garrido-Ramos MA, Utsunomia R, dos Santos RZ, Ezaz T,
1021 Deon GA, Porto-Foresti F, Liehr T, Cioffi MB. Independent evolution of satellite
1022 DNA
1023 sequences in homologous sex chromosomes of Neotropical armored catfish
1024 (*Harttia*). *Commun Biol*. 8:524.
1025 106. Sember A, Nguyen P, Perez MF, Altmanová M, Ráb P, Cioffi MB. 2021.
1026 Multiple sex chromosomes in teleost fishes from a cytogenetic perspective:
1027 state of the art and future challenges. *Philos Trans R Soc Lond B Biol Sci*.
1028 376:20200098.
1029 107. Simmons MP, Gatesy J. 2021. Collapsing dubiously resolved gene-tree
1030 branches in phylogenomic coalescent analyses. *Mol Phylogenet Evol.*
1031 158:107092.
1032 108. Sopniewski J, Shams F, Scheele BC, Kefford BJ, Ezaz T. 2019.
1033 Identifying sex-linked markers in *Litoria aurea*: a novel approach to
1034 understanding sex chromosome evolution in an amphibian. *Sci Rep*. 9:16591.
1035 109. Stamatakis A. 2014. RAxML version 8: a tool for phylogenetic analysis
1036 and post-analysis of large phylogenies. *Bioinformatics*. 30:1312-1313.
1037 110. Štundlová J, Hospodářská M, Lukšíková K, Voleníková A, Pavlica T,
1038 Altmanová M, Richter A, Reichard Mm, Dalíkova M, Pelikánová Š, et al. 2022.
1039 Sex chromosome differentiation via changes in the Y chromosome repeat
1040 landscape in African annual killifishes *Nothobranchius furzeri* and *N. kadleci*.
1041 *Chrom Res*. 30:309-333.

1042 111. Suchan T, Bataille CP, Reich MS, Toro-Delgado E, Vila R, Pierce NE,
1043 Talavera G. 2024. A trans-oceanic flight of over 4,200 km by painted lady
1044 butterflies. *Nature Commun*. 15:5205.
1045 112. Tagliacollo VA, Roxo FF, Duke-Sylvester SM, Oliveira C, Albert JS.
1046 2015. Biogeographical signature of river capture events in Amazonian lowlands.
1047 *J Biogeogr*. 42:2349-2362.
1048 113. Tiley GP, Poelstra JW, Dos Reis M, Yang Z, Yoder AD. 2020. Molecular
1049 clocks without rocks: new solutions for old problems. *Trends Genet*. 36: 845-
1050 856.
1051 114. Toups MA, Rodrigues N, Perrin N, Kirkpatrick M. 2019. A reciprocal
1052 translocation radically reshapes sex-linked inheritance in the common frog. *Mol*
1053 *Ecol.* 28:1877-1889.
1054 115. Trudeau VL. 2022. Neuroendocrine control of reproduction in teleost fish:
1055 concepts and controversies. *Annu Rev Anim Biosci*. 10:107-130.
1056 116. Van Doorn GS, Kirkpatrick M. 2007. Turnover of sex chromosomes
1057 induced by sexual conflict. *Nature*. 449:909-912.
1058 117. Wang D, Li Y, Li M, Yang W, Ma X, Zhang L, Wang Y, Feng Y, Zhang Y,
1059 Zhou R, et al. 2022. Repeated turnovers keep sex chromosomes young in
1060 willows. *Genome Biol*. 23:200
1061 118. Wang Y, Zhang RG, Hörandl E, Zhang ZX, Charlesworth D, He L. 2024.
1062 Evolution of sex-linked genes and the role of pericentromeric regions in sex
1063 chromosomes: insights from diploid willows. *Mol Biol Evol*. 41:msae235.
1064 119. Warmerdam DO, Wolthuis RM. 2019. Keeping ribosomal DNA intact: a
1065 repeating challenge. *Chrom Res*, 27:57-72.

1066 120. Wenzl P, Carling J, Kudrna D, Jaccoud D, Huttner E, Kleinhofs A, Kilian
1067 A. 2004. Diversity Arrays Technology (DArT) for whole-genome profiling of
1068 barley. *Proc Natl Acad Sci U S A*. 101:9915-9920.
1069 121. White MJD. 1940. The origin and evolution of multiple sex-chromosome
1070 mechanisms. *J Genet.* 40:303-336.
1071 122. Yang Z. 2015. The BPP program for species tree estimation and species
1072 delimitation. *Current Zool.* 61:854-865.
1073 123. Yannic G, Basset P, Hausser J. 2009. Chromosomal rearrangements
1074 and gene flow over time in an inter-specific hybrid zone of the *Sorex araneus*
1075 group. *Heredity*. 102:616-625.
1076 124. Yi X, Wang D, Reid K, Feng X, Löytynoja A, Merilä J. 2024. Sex
1077 chromosome turnover in hybridizing stickleback lineages. *Evol Lett*. 8:658-668.
1078 125. Yoshida K, Kitano J. 2012. The contribution of female meiotic drive to the
1079 evolution of neo-sex chromosomes. *Evolution*. 66:3198-3208.
1080 126. Zheng S, Tao H, Song Y, Li M, Yang H, Li J, Yan H, Sheraliev B, Tao W,
1081 Peng Z, et al. 2025. The origin, evolution, and translocation of sex
1082 chromosomes in *Silurus* catfish mediated by transposons. *BMC Biol*. 23:54.
1083 127. Zhu Z, Younas L, Zhou Q. 2025. Evolution and regulation of animal sex
1084 chromosomes. *Nat Rev Genet*. 26:59-74.

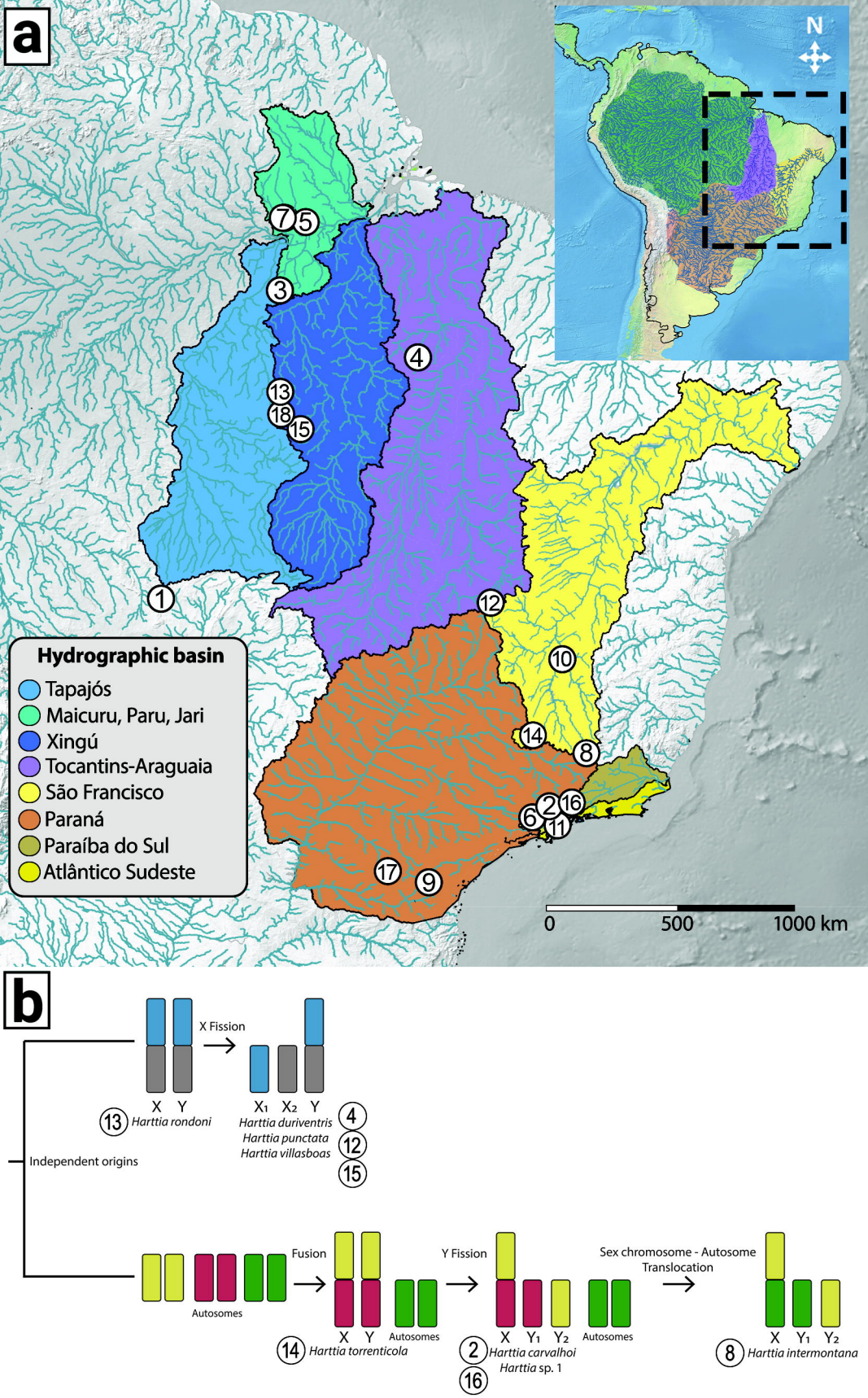
a
N
Hydrographic basin
Tapajós
Maicuru, Paru, Jari
Xingú
Tocantins-Araguaia
São Francisco
Paraná
Paraíba do Sul
Atlântico Sudeste
0
500
1000 km
b
X Fission
X Y
13 Harttia rondoni
X1 X2 Y
Harttia duriventris
Harttia punctata
Harttia villasboas
4
12
15
Independent origins
Autosomes
Fusion
X Y Autosomes
14 Harttia torrenticola
Y Fission
X Y1 Y2 Autosomes
2 Harttia carvalhoi
Harttia sp. 1
16
Sex chromosome - Autosome
Translocation
X Y1 Y2
8 Harttia intermontana

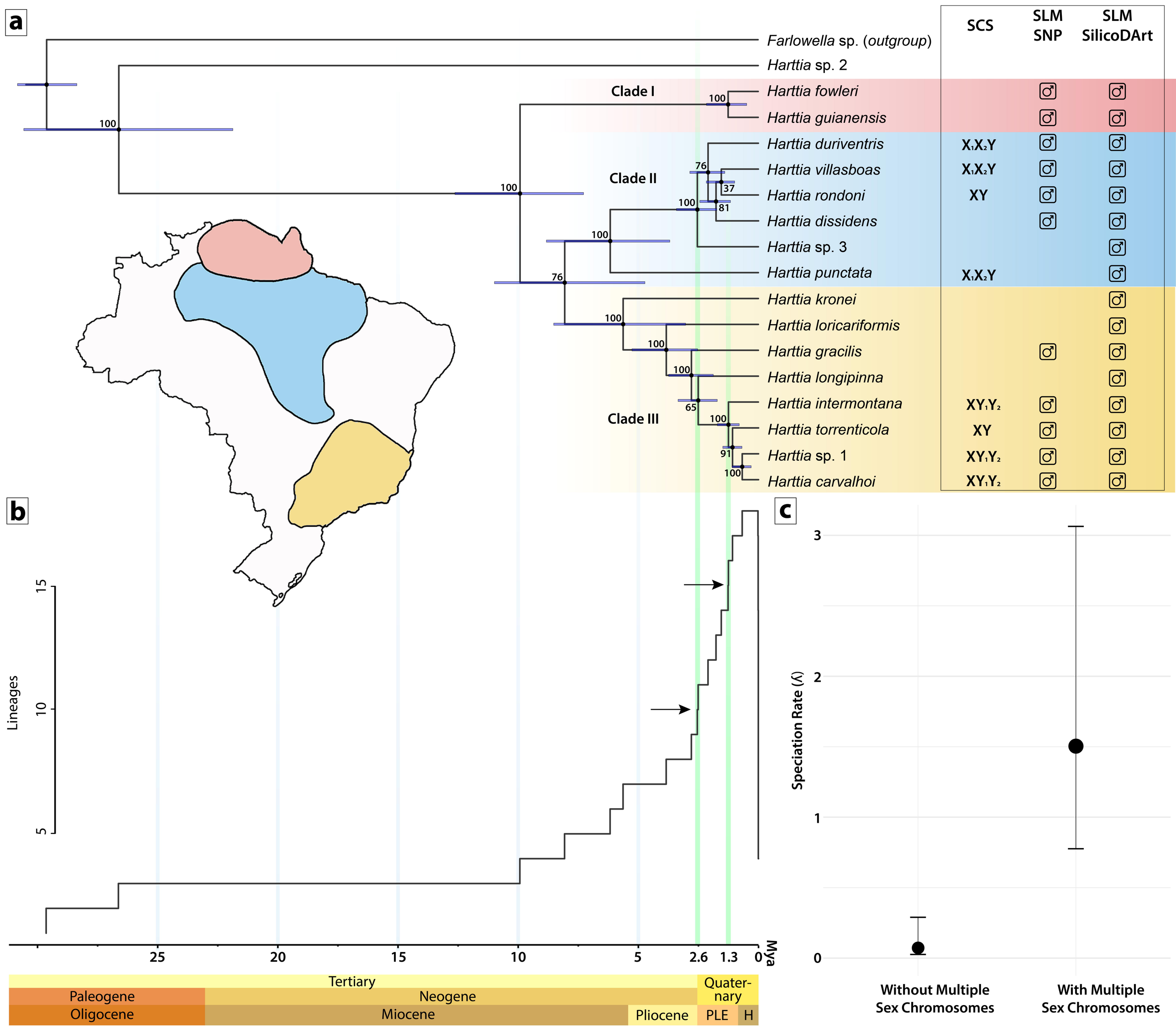
a
SCS
SLM SNP
SLM SilicoDArt
Farlowella sp. (outgroup)
Harttia sp. 2
Clade I
Harttia fowleri
Harttia guianensis
Clade II
Harttia duriventris X1X2Y
Harttia villasboas X1X2Y
Harttia rondoni XY
Harttia dissidens
Harttia sp. 3
Harttia punctata X1X2Y
Clade III
Harttia kronei
Harttia loricariformis
Harttia gracilis
Harttia longipinna
Harttia intermontana XY1Y2
Harttia torrenticola XY
Harttia sp. 1 XY1Y2
Harttia carvalhoi XY1Y2
100
76
37
81
65
91
b
Lineages
15
10
5
25
20
15
10
5
2.6
1.3
0
Mya
Tertiary
Quater-nary
Paleogene
Neogene
Oligocene
Miocene
Pliocene
PLE
H
c
Speciation Rate (λ)
3
2
1
0
Without Multiple Sex Chromosomes
With Multiple Sex Chromosomes

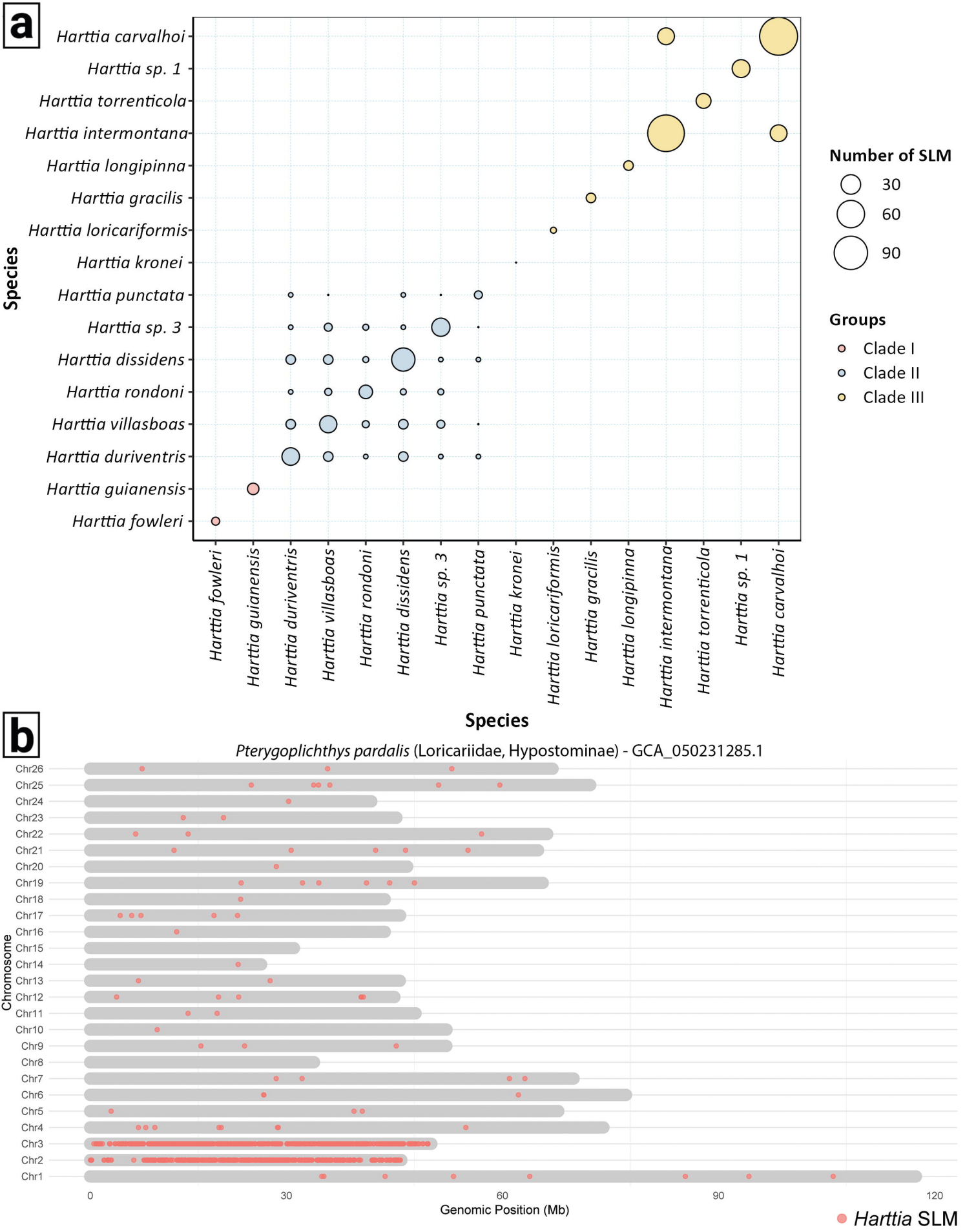
a
Harttia carvalhoi
Harttia sp. 1
Harttia torrenticola
Harttia intermontana
Harttia longipinna
Harttia gracilis
Harttia loricariformis
Harttia kronei
Harttia punctata
Harttia sp. 3
Harttia dissidens
Harttia rondoni
Harttia villasboas
Harttia duriventris
Harttia guianensis
Harttia fowleri
Species
Number of SLM
30
60
90
Groups
Clade I
Clade II
Clade III
b
Pterygoplichthys pardalis (Loricariidae, Hypostominae) - GCA_050231285.1
Chromosome
Chr26
Chr25
Chr24
Chr23
Chr22
Chr21
Chr20
Chr19
Chr18
Chr17
Chr16
Chr15
Chr14
Chr13
Chr12
Chr11
Chr10
Chr9
Chr8
Chr7
Chr6
Chr5
Chr4
Chr3
Chr2
Chr1
0
30
60
90
120
Genomic Position (Mb)
Harttia SLM

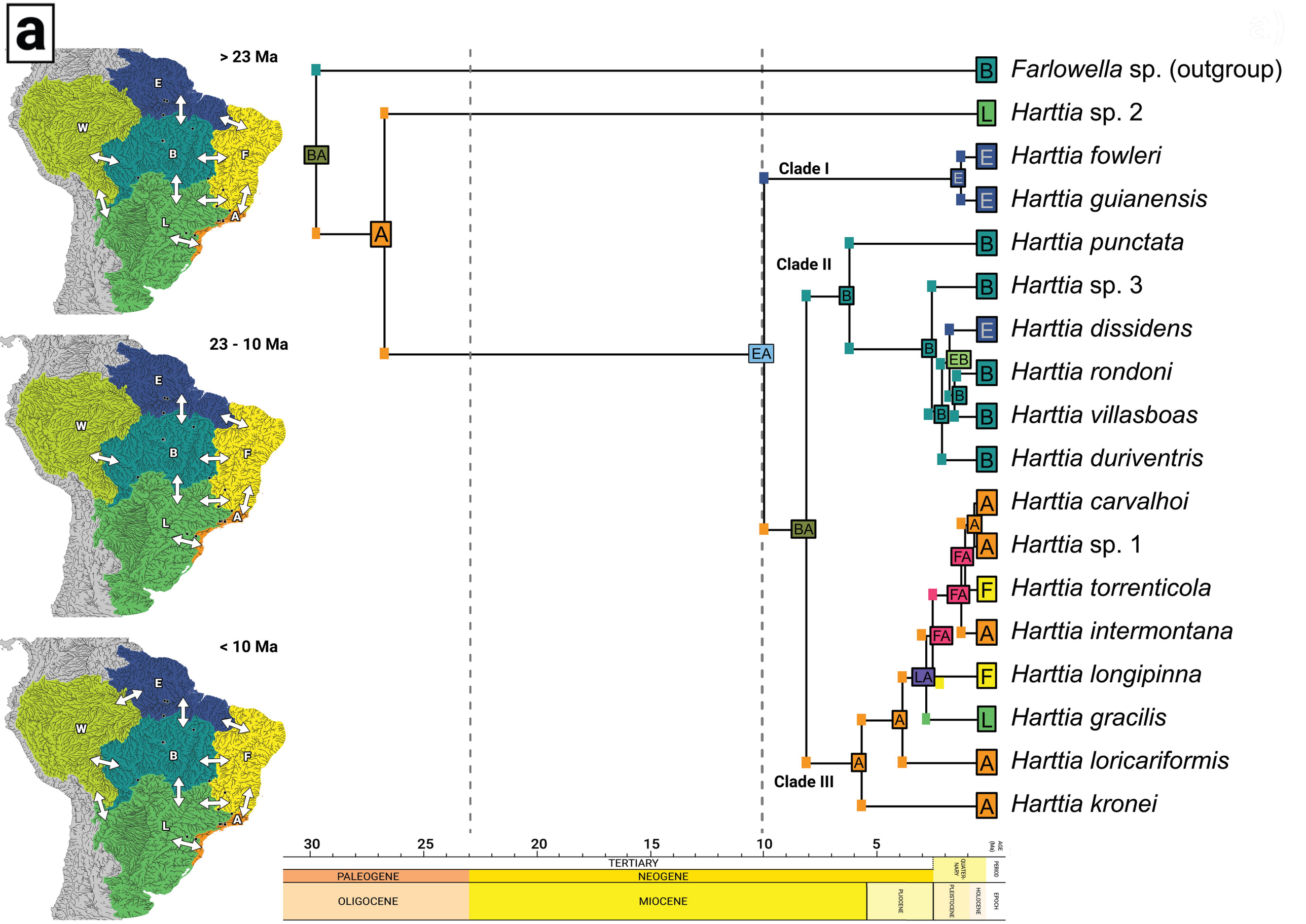
a
> 23 Ma
23 - 10 Ma
< 10 Ma
E
W
B
F
L
A
BA
EA
LA
FA
Clade I
Clade II
Clade III
Farlowella sp. (outgroup)
Harttia sp. 2
Harttia fowleri
Harttia guianensis
Harttia punctata
Harttia sp. 3
Harttia dissidens
Harttia rondoni
Harttia villasboas
Harttia duriventris
Harttia carvalhoi
Harttia sp. 1
Harttia torrenticola
Harttia intermontana
Harttia longipinna
Harttia gracilis
Harttia loricariformis
Harttia kronei
30
25
20
15
10
5
AGE (Ma)
TERTIARY
PALEOGENE
NEOGENE
QUATERNARY
PERIOD
OLIGOCENE
MIOCENE
PLIOCENE
PLEISTOCENE
HOLOCENE
EPOCH

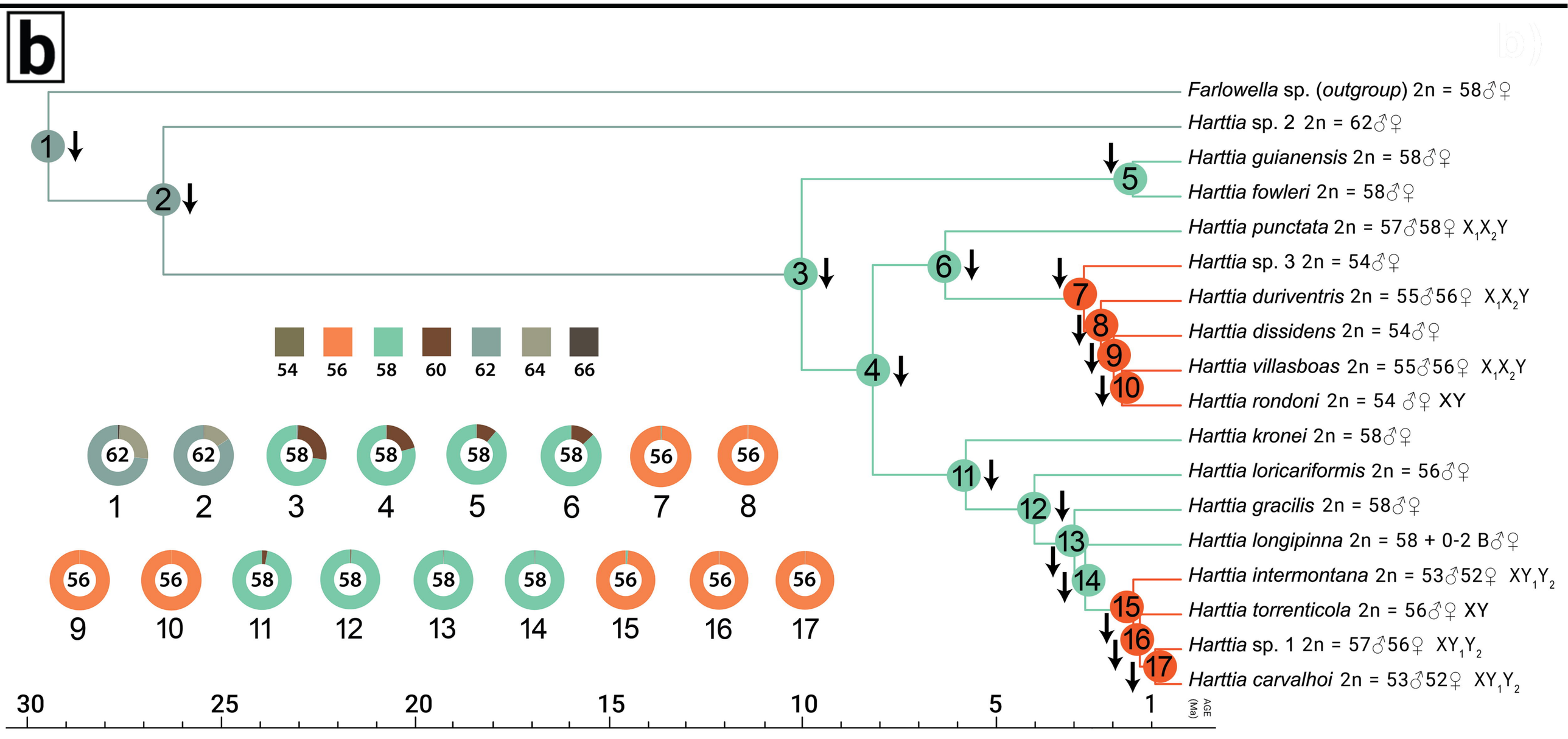
b
Farlowella sp. (outgroup) 2n = 58♂♀
Harttia sp. 2 2n = 62♂♀
Harttia guianensis 2n = 58♂♀
Harttia fowleri 2n = 58♂♀
Harttia punctata 2n = 57♂58♀ X1X2Y
Harttia sp. 3 2n = 54♂♀
Harttia duriventris 2n = 55♂56♀ X1X2Y
Harttia dissidens 2n = 54♂♀
Harttia villasboas 2n = 55♂56♀ X1X2Y
Harttia rondoni 2n = 54 ♂♀ XY
Harttia kronei 2n = 58♂♀
Harttia loricariformis 2n = 56♂♀
Harttia gracilis 2n = 58♂♀
Harttia longipinna 2n = 58 + 0-2 B♂♀
Harttia intermontana 2n = 53♂52♀ XY1Y2
Harttia torrenticola 2n = 56♂♀ XY
Harttia sp. 1 2n = 57♂56♀ XY1Y2
Harttia carvalhoi 2n = 53♂52♀ XY1Y2
54
56
58
60
62
64
66
30
25
20
15
10
5
1
AGE (Ma)

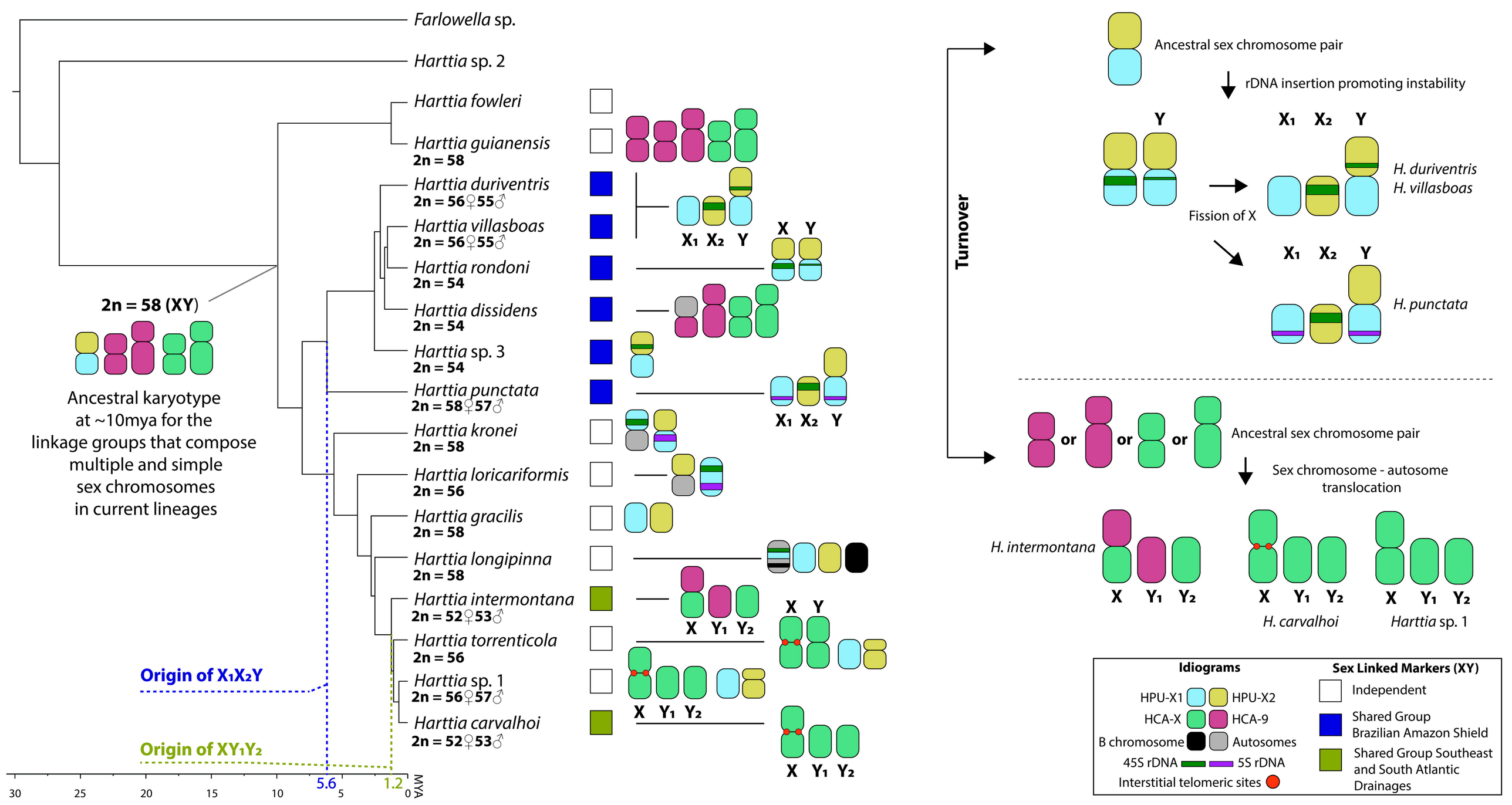
Farlowella sp.
Harttia sp. 2
Harttia fowleri
Harttia guianensis
2n = 58
Harttia duriventris
2n = 56♀55♂
Harttia villasboas
2n = 56♀55♂
Harttia rondoni
2n = 54
Harttia dissidens
2n = 54
Harttia sp. 3
2n = 54
Harttia punctata
2n = 58♀57♂
Harttia kronei
2n = 58
Harttia loricariformis
2n = 56
Harttia gracilis
2n = 58
Harttia longipinna
2n = 58
Harttia intermontana
2n = 52♀53♂
Harttia torrenticola
2n = 56
Harttia sp. 1
2n = 56♀57♂
Harttia carvalhoi
2n = 52♀53♂
2n = 58 (XY)
Ancestral karyotype at ~10mya for the linkage groups that compose multiple and simple sex chromosomes in current lineages
Origin of X1X2Y
Origin of XY1Y2
30
25
20
15
10
5
0
MYA
5.6
1.2
X1 X2 Y
X Y
X1 X2 Y
X Y1 Y2
X Y
X Y1 Y2
X Y1 Y2
Turnover
Ancestral sex chromosome pair
rDNA insertion promoting instability
Y
X1 X2 Y
H. duriventris
H. villasboas
Fission of X
X1 X2 Y
H. punctata
or
or
or
Ancestral sex chromosome pair
Sex chromosome - autosome translocation
H. intermontana
X Y1 Y2
X Y1 Y2
H. carvalhoi
X Y1 Y2
Harttia sp. 1
Idiograms
HPU-X1
HPU-X2
HCA-X
HCA-9
B chromosome
Autosomes
45S rDNA
5S rDNA
Interstitial telomeric sites
Sex Linked Markers (XY)
Independent
Shared Group Brazilian Amazon Shield
Shared Group Southeast and South Atlantic Drainages